*Annals of Botany* **121**: 1107–1125, 2018
doi: 10.1093/aob/mcy005, available online at www.academic.oup.com/aob

ANNALS OF BOTANY
Founded 1887

INVITED REVIEW

# The cell biology of secondary cell wall biosynthesis

**Miranda J. Meents, Yoichiro Watanabe and A. Lacey Samuels***

*Department of Botany, University of British Columbia, 6270 University Blvd., Vancouver, BC, Canada, V6T 1Z4*
**For correspondence. E-mail lsamuels@mail.ubc.ca*

Received: 14 August 2017 Returned for revision: 24 October 2017 Editorial decision: 2 January 2018 Accepted: 16 January 2018
Published electronically 5 February 2018

• **Background** Secondary cell walls (SCWs) form the architecture of terrestrial plant biomass. They reinforce tracheary elements and strengthen fibres to permit upright growth and the formation of forest canopies. The cells that synthesize a strong, thick SCW around their protoplast must undergo a dramatic commitment to cellulose, hemicellulose and lignin production.
• **Scope** This review puts SCW biosynthesis in a cellular context, with the aim of integrating molecular biology and biochemistry with plant cell biology. While SCWs are deposited in diverse tissue and cellular contexts including in sclerenchyma (fibres and sclereids), phloem (fibres) and xylem (tracheids, fibres and vessels), the focus of this review reflects the fact that protoxylem tracheary elements have proven to be the most amenable experimental system in which to study the cell biology of SCWs.
• **Conclusions** SCW biosynthesis requires the co-ordination of plasma membrane cellulose synthases, hemicellulose production in the Golgi and lignin polymer deposition in the apoplast. At the plasma membrane where the SCW is deposited under the guidance of cortical microtubules, there is a high density of SCW cellulose synthase complexes producing cellulose microfibrils consisting of 18–24 glucan chains. These microfibrils are extruded into a cell wall matrix rich in SCW-specific hemicelluloses, typically xylan and mannan. The biosynthesis of eudicot SCW glucuronoxylan is taken as an example to illustrate the emerging importance of protein–protein complexes in the Golgi. From the *trans*-Golgi, trafficking of vesicles carrying hemicelluloses, cellulose synthases and oxidative enzymes is crucial for exocytosis of SCW components at the microtubule-rich cell membrane domains, producing characteristic SCW patterns. The final step of SCW biosynthesis is lignification, with monolignols secreted by the lignifying cell and, in some cases, by neighbouring cells as well. Oxidative enzymes such as laccases and peroxidases, embedded in the polysaccharide cell wall matrix, determine where lignin is deposited.

**Key words:** Secondary cell wall, cellulose, hemicellulose, lignin, cell biology, trafficking.

## INTRODUCTION

The emergence of lignified secondary cell walls (SCWs) is one of the most important evolutionary events allowing plants to dominate the terrestrial environment. These strong and rigid walls provide physical support for the plant and reinforce conduits for long-distance transport in the xylem. While tracheary elements (i.e. vessels and tracheids) play key physiological roles in water and mineral transport, the bulk of the world's SCW biomass is in the form of fibres in secondary xylem (i.e. xylary fibres) and in primary growth (i.e. sclerenchymous fibres) (Fig. 1). Although only a sub-set of cells in any given plant form SCWs, in many woody plants, such as trees, the majority of the plant's mass is composed of SCWs in the form of fibres, tracheids and vessels.

The woody tissues of plants are important for human cultures and economies. Globally, wood is burned for fuel, used in construction of buildings and furnishings, in the production of paper and fibres, and carved to make tools and art. More recently, the lignocellulosic biomass of SCWs has been targeted as a resource for renewable biofuels. The degree to which this resource can be exploited is largely determined by the ultrastructure and chemistry of the SCWs produced by plants. This chemistry has the capacity to affect the inherent recalcitrance of SCWs to biochemical processing for biofuel production, and therefore the economic viability of second-generation biofuels (Marriott *et al.*, 2016). SCWs could also be exploited by repurposing agriculture or forestry waste by-products rich in lignin into value-added products (Ragauskas *et al.*, 2014). A thorough understanding of the SCW and how it is produced will allow identification and tailoring of wall compositions that are optimal for these types of industrial processes.

Classically, SCWs are strong, thickened cell walls defined by being deposited after the plant cell has finished its expansion. In contrast, primary cell walls (PCWs) are defined as the walls formed during cell expansion that resist the forces exerted by turgor pressure, and are flexible and extensible enough to facilitate morphogenesis. These classical definitions generally correlate with characteristic cell wall chemical compositions; however, exceptions are found. For example, the arabidopsis seed coat epidermis has a specialized cell wall that is laid down after the cell has finished expansion, so classically should be considered a secondary cell wall, but compositionally it is similar to the primary wall as it is pectin and xyloglucan rich (Haughn and Western, 2012). Another exception to the classical definition includes fibres from fescue (*Festuca arundinacea*

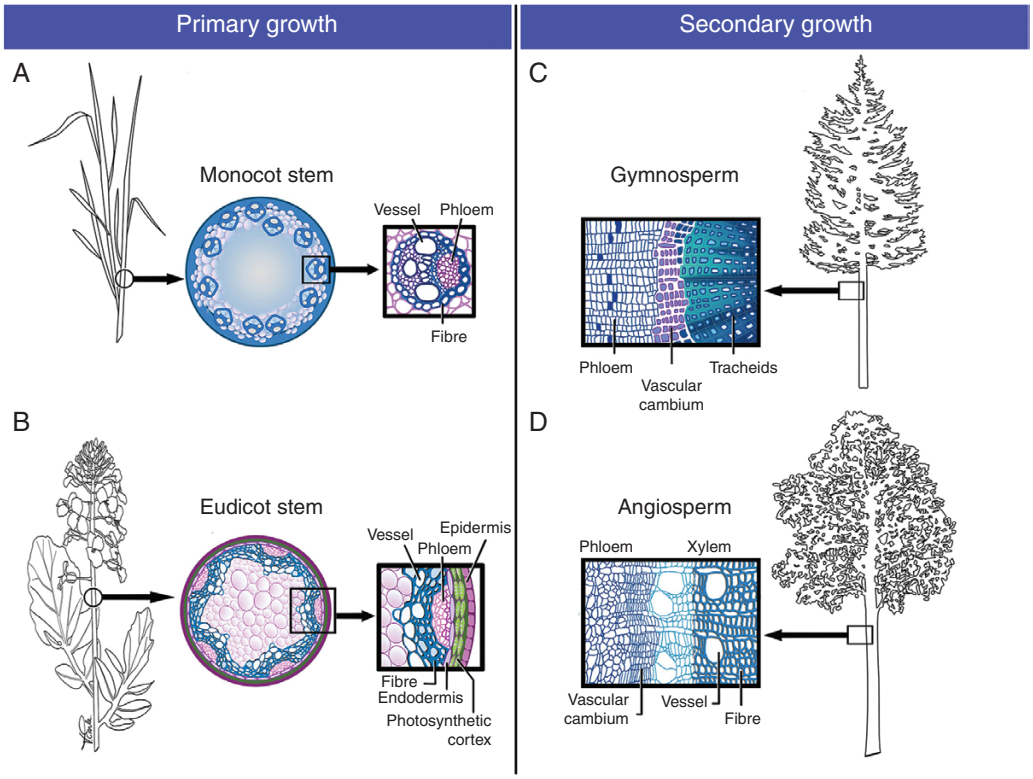


FIG. 1. SCWs in primary and secondary stem growth. Illustrative examples of SCWs in water-conducting cells (vessels, tracheids) and supportive fibres. (A and B) SCWs in primary growth. (A) SCWs in monocot primary growth exemplified in a cross-section of a grass stem internode where vascular bundles with large metaxylem vessels are encased in SCW-rich sclerenchyma (e.g. Brachypodium). (B) SCWs in eudicot primary growth illustrated in a stem cross-section prior to onset of secondary thickening (e.g. Brassica). SCWs are found in the vascular vessels and fibres, which are continuous with the thick interfascicular fibres. (C and D) SCWs in secondary growth, marked by the presence of the vascular cambium. (C) Gymnosperm secondary growth showing thick SCWs in the water-conducting and supportive tracheids of the secondary xylem (e.g. Pinus). (D) Angiosperm secondary growth showing SCWs in the water-conducting vessels and the supportive fibres (e.g. Populus).

Schreb.) leaf blades, where SCW deposition occurs in conjunction with expansion (MacAdam and Nelson, 2002).

The goal of this review is to examine SCW biosynthesis in a cell biology context, with emphasis on how the protoplast produces large amounts of the SCW components, how they are secreted and how the precise patterns of SCWs are generated. This activity takes place in SCW-producing cells derived from procambium in axially growing organs, from the vascular cambium in wood formation or in extraxylary fibres arising from ground tissue (Fig. 1), with common mechanisms within the protoplast driving SCW production in each case. As the cell shifts production from PCW to SCW biosynthesis, the entire cell wall biosynthetic machinery is remodelled in response to transcriptomic cascades in tracheids, fibres or vessels (reviewed in Taylor-Teeples *et al.*, 2014; Nakano *et al.*, 2015). A new set of cellulose synthase (CESA) enzymes are produced and trafficked to the cell surface, accompanied by rearrangements of the cytoskeleton. The types of cell wall matrix polysaccharides being made in the Golgi switch (e.g. in eudicots, from pectin and xyloglucan rich to glucuronoxylan rich), and secretion is focused to SCW domains. Typically, the final step of SCW synthesis is the deposition of polyphenolic lignin in the polysaccharide matrix. The remodelling of the cell during SCW production occurs in an overlapping series of events: the transition from PCW to SCW, SCW synthesis dominated by polysaccharide production, SCW maturation dominated by lignification and often co-occurring with programmed cell death (Fig. 2). As with the strict definition of SCW, exceptions to this sequence abound, such as the gelatinous type of SCW exemplified by bast fibres which are high in cellulose but lacking lignin (Gorshkova *et al.*, 2012).

## CELLULOSE

Cellulose is the most abundant biopolymer on earth, with an estimated annual production of $10^{10}$–$10^{11}$ t (Hon, 1994). The majority of this cellulose is produced in the SCWs of terrestrial plants, as it comprises up to 60 % of the SCW, compared with 20–30 % in PCWs (reviewed in McNeil *et al.*, 1984). Cellulose is composed of linear chains of β-(1–4) glucans, which aggregate to form highly crystalline cellulose microfibrils that are held together by many intra- and intermolecular hydrogen bonds and Van der Waals forces (Kim *et al.*, 2013). The overall structure of cellulose microfibrils differs between PCWs and SCWs, most notably with a higher crystallinity and degree of polymerization in SCWs affecting its strength and rigidity (McNeil *et al.*, 1984). Despite this importance, the cellular and enzymatic mechanisms controlling these features of cellulose microfibrils remain poorly understood. Here we discuss recent advancements in our understanding of the CESA enzymes and the cellular mechanisms influencing their activity during SCW biosynthesis.

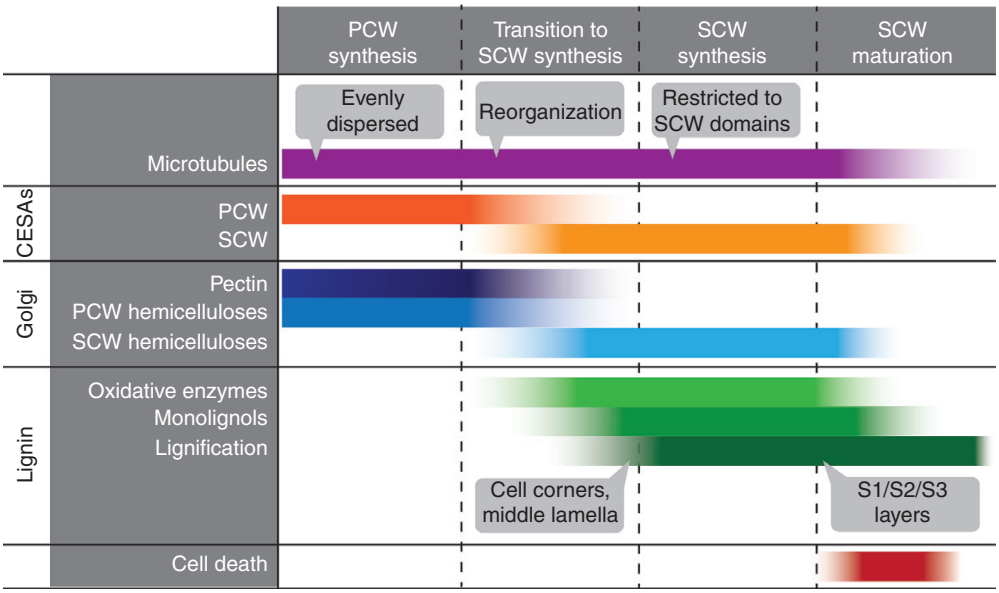


FIG. 2. The onset and completion of secondary cell wall (SCW) synthesis involves changes in many cellular processes. The transition from primary cell wall (PCW) to SCW deposition encompasses reorganization of microtubules, an exchange of primary cellulose synthases (CESAs) for specialized secondary CESAs and a shift in Golgi production from primary wall pectins and hemicelluloses (e.g. xyloglucan and arabinoxylans) to secondary wall hemicelluloses (e.g. xylans and mannans). Lignification occurs later in SCW production, though the lignin monomers (monolignols) and oxidative enzymes (e.g. laccases and peroxidases) required for their polymerization may be synthesized and secreted earlier. Cells that are dead at maturity undergo programmed cell death, after which lignification may continue using monolignols produced by neighbouring parenchyma.

*SCW cellulose biosynthetic enzymes*

Cellulose is synthesized by CESA enzymes in the plasma membrane (reviewed by McFarlane *et al.*, 2014). Each CESA is hypothesized to synthesize a single glucan chain by polymerizing glucose derived from cytosolic UDP-glucose. This hypothesis is strongly supported by X-ray crystallography studies of the BcsA–BcsB cellulose synthase complex of the bacterium *Rhodobacter sphaeroides*, in which BcsA was physically associated with one glucan chain (Morgan *et al.*, 2013). This demonstrated that each CESA enzyme has the catalytic structure necessary to carry out polymerization (Morgan *et al.*, 2013; Omadjela *et al.*, 2013). Although the crystal structure of plant CESAs remains to be resolved, computationally predicted structures of a cotton SCW CESA modelled on the bacterial CESA suggest that plant and bacterial CESAs have similar features, further supporting a one CESA–one glucan chain model (Slabaugh *et al.*, 2014; Sethaphong *et al.*, 2015).

The number of *CESA* genes varies among plant species, with different sets of CESAs required for cellulose synthesis in PCWs and SCWs (Carroll and Specht, 2011). In arabidopsis, for example, CESA1, CESA3 and one of CESA2/5/6/9 are required for PCW production, while CESA4, CESA7 and CESA8 are needed for SCW production (Persson *et al.*, 2005). The CESAs involved in SCW synthesis were first identified in knock-out mutants in arabidopsis by their characteristic irregular xylem (*irx*) phenotype in arabidopsis stem sections (Turner and Somerville, 1997), now considered a diagnostic phenotype for SCW disruption of many kinds. The knock-out alleles, *cesa4*$^{irx5}$, *cesa7*$^{irx3}$ and *cesa8*$^{irx1}$, had approx. 70 % less cellulose than wild-type plants (Taylor *et al.*, 1999, 2000, 2003). However, not all SCW CESA mutants have an irregular xylem phenotype. The missense fragile fibre (*fra*) mutants, *cesa7*$^{fra5}$ and *cesa8*$^{fra6}$, have normal vessels but reduced SCW thickness in fibres and a significant decrease in cellulose content (Zhong *et al.*, 2003). Mutations in SCW CESAs can also affect PCW components, as the missense mutant *cesa7*$^{mur10}$ has altered pectin and xyloglucan structures, predicted to be a result of perturbed cell wall integrity signalling (Bosca *et al.*, 2006). Expression analyses using either antibodies raised against the class-specific region unique to each SCW CESA or green fluorescent protein (GFP) tagging of CESA revealed that CESA4, CESA7 and CESA8 are present at the same time in developing tracheary xylem and interfascicular fibres (Gardiner *et al.*, 2003; Taylor *et al.*, 2003). This combination of expression patterns and mutant phenotypes strongly suggests that these proteins synthesize cellulose for SCWs.

*CESA complex (CSC) formation and function*

Although each CESA is believed to be capable of glucan synthesis independently, *in planta* cellulose is synthesized at the plasma membrane by a multiprotein complex called the cellulose synthase complex (CSC). Freeze-fracture/transmission electron microscopy (TEM) or negative staining/TEM of various moss and vascular plant plasma membranes showed hexameric rosette structures approx. 25 nm in diameter on the extracellular face, with a larger 40 nm globular structure on the cytosolic face (Giddings *et al.*, 1980; Mueller and Brown, 1980; Bowling and Brown, 2008). In freeze-fracture images of xylem vessels from *Lepidium sativum* roots, rosettes were only seen in domains where the SCW is forming (Herth, 1985). Antibody labelling against the catalytic domain of CESAs confirmed that the rosettes seen in freeze-fracture/TEM in developing cotton fibres did indeed contain CESA proteins (Kimura *et al.*, 1999),

verifying the interpretation that a rosette corresponds to a single CSC. Historically, it was believed that ≥36 CESAs made up a complete CSC, based on the number of chains that would account for the observed microfibril widths and the 6-fold symmetry of rosettes (McFarlane *et al.*, 2014). However, recent studies using improved analytical techniques and computational modelling have shown that CSCs are more likely to be composed of either 18 CESAs (Newman *et al.*, 2013; Oehme *et al.*, 2015; Nixon *et al.*, 2016; Vandavasi *et al.*, 2016) or 24 CESAs (Fernandes *et al.*, 2011; Thomas *et al.*, 2013; Oehme *et al.*, 2015). As such, the emerging model of the CSC is a hexamer of CESA trimers or tetramers, producing 18–24 β-(1–4) glucan chains that assemble into a microfibril.

Each CSC must also contain a mix of at least three types of CESA proteins. Co-immunoprecipitation (CoIP) experiments demonstrated that when one of the three CESAs is lost, the large CSC complex is no longer detected, the remaining two CESAs no longer interact and they accumulate to lower levels compared with the wild type. This was the case in both PCW CESAs (Desprez *et al.*, 2007) and SCW CESAs (Taylor *et al.*, 2003). Furthermore, quantitative western blots, and CoIP followed by mass spectrometry quantification, have suggested that the three CESA classes have a stoichiometric ratio of 1:1:1 within a complex (Gonneau *et al.*, 2014; Hill *et al.*, 2014). Interestingly, null mutants of SCW *CESA* genes are still able to produce some cellulose, albeit with altered crystallinity and lower abundance (Taylor *et al.*, 2003). It may be that the other classes of CESA can partially compensate for the absent CESA class. This is supported by studies showing partial complementation of an SCW *cesa8* mutant by an ectopically driven PCW CESA1, and of a PCW *cesa3* mutant by SCW CESA7 (Carroll *et al.*, 2012). Alternatively, the remaining CESAs may form aberrant CSCs or act as monomers, producing cellulose of lower quality on their own (Arioli *et al.*, 1998). Heterologous expression of a single *Populus trichocarpa* SCW CESA, *Ptt*CESA8, in the yeast *Pichia pastoris* resulted in the formation of protein complexes and cellulose microfibril production (Purushotham *et al.*, 2016). In yeast expressing *Ptt*CESA8 with N-terminal truncations, microfibrils were not formed, though production of cellulose chains continued (Purushotham *et al.*, 2016). As the N-terminus is a region important in CESA–CESA interactions, this indicates that CSC formation is required for aggregation of cellulose into microfibrils.

It is not currently understood why multiple CESA isoforms are needed to form a complete CSC or why different CESAs appear to have distinct functions. Genomic analysis of several plant species revealed that the specialization of CESA classes has persisted through much of the evolution of land plants (Carroll and Specht, 2011). Primary amino acid sequence comparisons indicate that the hypervariable and class-specific regions of CESAs are more conserved among orthologues than paralogues, leading to the hypothesis that the conserved amino acids within a class of CESAs reflect functional specialization (Pear *et al.*, 1996; Doblin, 2002). Part of this specialization may be conferred by phosphorylation, as these regions contain several highly conserved phosphorylation sites, which have been shown with site-directed mutagenesis and phosphorylation assays to be involved in regulating CESA activity (Taylor, 2007; Chen *et al.*, 2010, 2016; Sánchez-Rodríguez *et al.*, 2017). However, other domains such as the far N-terminus and C-terminus contain sequences that are highly conserved in some CESA classes but lost in others, implying that specificity may extend beyond the previously proposed regions (Carroll and Specht, 2011). Recent work creating a comprehensive set of hybrid SCW CESAs, in which several domains from the three SCW CESAs in arabidopsis were swapped and then tested for complementation of SCW *cesa* mutants, showed that class specificity was not dependent on either the class-specific or the hypervariable domains (Kumar *et al.*, 2017). Instead, the suite of CESAs may be required because each CESA isoform has a specific location and fit within the complex (Wang *et al.*, 2006; Kumar *et al.*, 2017). Analyses of chimeric PCW CESAs have shown that when the C-terminal half of CESA3 is fused to the N-terminal half of CESA1 and transformed into *cesa1*$^{rsw1}$ mutants, a dominant-negative effect on plant growth was found, implying that the non-functional chimeric protein was occupying the site of the normal functioning CESAs (Wang *et al.*, 2006). The hybrid SCW CESA swapping experiments show that CESA8 is most accepting of other CESA domains, suggesting that it may have a peripheral position in the complex, while CESA7 was the least accepting of other CESA domains, implying that it may be in a more constrained position (Kumar *et al.*, 2017). Still, it is difficult to conclude that the multiple isoforms exist to play structural roles in a complete CSC until we have a higher resolution view of how each CESA interacts with its partners.

Assembly of CSCs from the CESA monomers is believed to occur in the Golgi apparatus (Haigler and Brown, 1986). Although rosettes have been observed in the endoplasmic reticulum (ER) in a single freeze-fracture image (Rudolph, 1987), little additional evidence suggests that complex formation begins here. Indeed, other freeze-fracture imaging (Haigler and Brown, 1986) and fluorescent microscopy of tagged PCW and SCW CESAs (Paredez *et al.*, 2006; Wightman and Turner, 2008; Crowell *et al.*, 2009; Gutierrez *et al.*, 2009; Watanabe *et al.*, 2015) have not detected rosettes or significant CESA fluorescent label in pre-Golgi compartments. Further evidence for complex formation in the Golgi comes from analysis of the Golgi-localized STELLO proteins (Zhang *et al.*, 2016). STELLOs were shown to interact with PCW and SCW CESAs in the Golgi, and the STELLO double mutant had altered distribution of CESAs in the Golgi, a reduction in PCW and SCW CSC formation, decreased PCW CSC delivery to the plasma membrane and altered CSC velocity (Zhang *et al.*, 2016). This highlights the importance of the Golgi in CSC formation, and provides evidence that proper complex formation affects the function of the CESAs at the plasma membrane. However, it is still unclear how STELLOs might mediate CESA complex formation in the Golgi and if other proteins are involved.

### *Biosynthesis of cellulose at the plasma membrane*

The dynamics of cellulose synthesis at the plasma membrane is another area of cellulose biology that has been extensively investigated. Fluorescently-tagged PCW CESAs in CSCs have been shown to move through the plasma membrane (Paredez *et al.*, 2006). This movement is thought to be powered by the polymerizing activity of the CSCs pushing against the newly synthesized cellulose microfibril embedded in the

wall (Herth, 1980; DeBolt *et al.*, 2007; Diotallevi and Mulder, 2007). Imaging of fluorescently tagged PCW CSCs showed that they move in linear, bi-directional trajectories at speeds of 70–500 nm $min^{-1}$, which has been proposed to correspond to 300–1000 glucose molecules $min^{-1}$ (Paredez *et al.*, 2006). CSC speeds increase at higher temperatures, a property that has been proposed to regulate the growth rate of the cell (Fujita *et al.*, 2011). All of these measurements of PCW CESA velocities were taken in the epidermal cells of arabidopsis hypocotyls using spinning-disk confocal microscopy; direct measurement of SCW CESA is challenging as native tracheary elements are deep within plants, not on the surface (Wightman and Turner, 2008; Wightman *et al.*, 2009).

One solution to the challenge of SCW CESA imaging was to visualize fluorescently tagged SCW CESAs in transdifferentiating SCW-producing protoxylem cells (Watanabe *et al.*, 2015). By inducing xylem cell fate in epidermal cells of arabidopsis, SCW CESAs were directly imaged, demonstrating their intense accumulation in plasma membrane domains adjacent to forming SCWs and depletion in other plasma membrane regions. These domains also closely co-localized with bundles of cortical microtubules, which were previously shown to mark areas of SCW deposition (Hepler and Fosket, 1971; Gardiner *et al.*, 2003; Wightman and Turner, 2008). The restriction of CSCs to SCW regions leads to a significantly higher density of CSCs than is seen in PCW production (Watanabe *et al.*, 2015). Clusters of CSCs have been observed to move in co-ordinated trajectories along a single track, which leads to the large aggregations of highly ordered cellulose microfibrils that are seen in SCW domains and not PCWs (S. Li *et al.*, 2016). Thus, the high density and tightly co-ordinated tracking of CSCs in SCW domains (Fig. 3) plays a key role in forming the thickened, cellulose-rich SCWs in developing xylem cells.

The localization of CSCs in SCW domains of developing xylem cells has been found to be dependent on CESA acylation (Kumar *et al.*, 2016*b*). Such post-translational modifications have been proposed to increase the hydrophobicity of the CESAs, increasing their association with the plasma membrane lipids and ensuring CSCs remain in the plasma membrane as the cellulose pushes the CSC down, depressing the membrane (Diotallevi and Mulder, 2007; Kumar *et al.*, 2016*b*). The addition of acyl-groups to the CESAs may facilitate formation of lipid microdomains that have been hypothesized to be crucial for CSC function (Guerriero *et al.*, 2010; Kumar *et al.*, 2016*b*). Cells with patterned SCW deposition provide an opportunity to test if the membrane environment around CSCs differs from the rest of the plasma membrane. The high density of SCW CSCs should enrich any associated membrane features in the SCW domains, which would then be distinct from the other membrane domains that lack CSCs.

The length of the cellulose chains in the wall (degree of polymerization) has been linked to both the speed of CSCs and the lifetime of a CSC at the plasma membrane (Bashline *et al.*, 2014). If lifetime determines degree of cellulose polymerization, then we would expect the pool of SCW CESAs to have a longer half-life, as cellulose in SCWs is usually greater than three times longer than in PCWs (McNeil *et al.*, 1984). Due to the high density of CSCs at the plasma membrane, and the difficulty in tracking a particle travelling the circumference of the cell, the lifetime of CSCs at the plasma membrane has not been directly measured. The lifetime at the plasma membrane of PCW CSCs was indirectly estimated to be about 21 min, based on freeze-fracture experiments of the moss *Funaria*

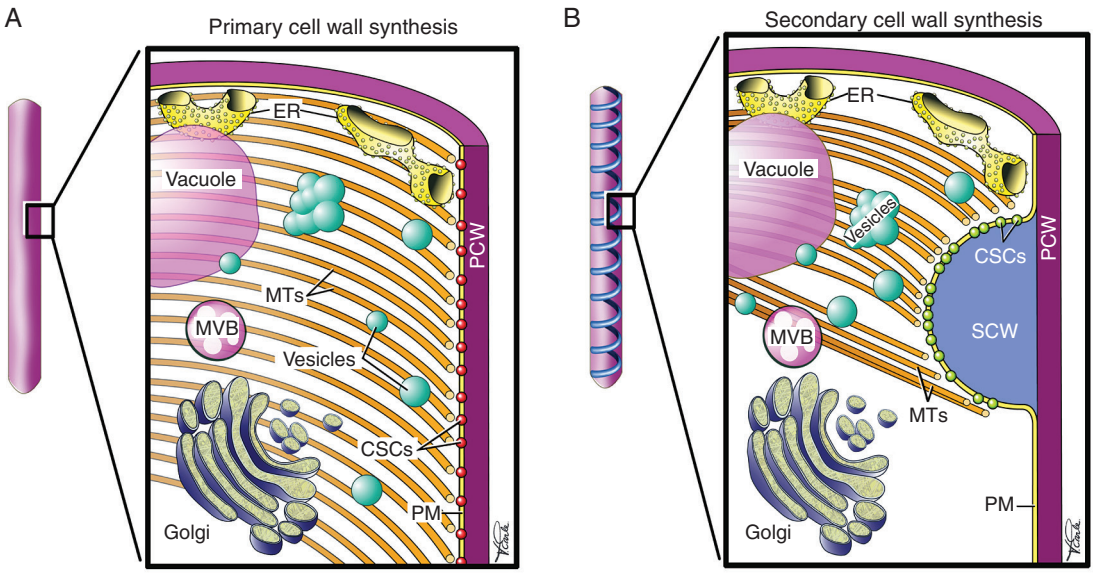


FIG. 3. Cellular changes accompanying SCW biosynthesis. (A) Part of a developing protoxylem tracheary element prior to SCW deposition (left) is seen in cross-section (right). Primary CESA complexes (CSCs) (red) in the plasma membrane (PM) produce cellulose for the primary cell wall (PCW). Accompanied secretory vesicles (turquoise) deliver hemicelluloses, pectins and glycoproteins to the wall by fusing with the PM. Microtubules (MTs) are widely dispersed and run roughly perpendicular to the long axis of the cell. Also shown are the endoplasmic reticulum (ER), a multivesicular body (MVB) and the vacuole. (B) Production of SCWs in protoxylem results in a helical SCW (left). A cross-section of a single SCW thickening (right) shows that microtubules have become bundled and line the PM at the region of SCW formation. A dense population of secondary wall CSCs (green) are restricted to the SCW domain. Vesicles traffic CSCs and deliver hemicelluloses (e.g. xylan and mannan) and glycoproteins (e.g. laccases) to the SCW.

*hygrometrica* after treatment with monensin, an inhibitor of the Golgi-mediated secretion pathway (Rudolph and Schnepf, 1988). These values are comparable with the estimated lifetime of 5–20 min from live-cell imaging of PCW CSC delivery and densities at the plasma membrane (Bashline *et al.*, 2013; Sampathkumar *et al.*, 2013). In western blot analysis, levels of the cotton (*Gossypium hirsutum*) SCW *Gh*CESA1 rapidly declined after protein synthesis inhibition by cycloheximide, while other membrane proteins persisted for well over 4 h (Jacob-Wilk *et al.*, 2006). The authors estimated that the SCW CESAs have a half-life of <30 min. These estimates all support the view of CESAs as actively turning over in both PCWs and SCWs, consistent with the large population of intracellular CESAs seen in live-cell imaging (Wightman and Turner, 2008; Crowell *et al.*, 2009; Gutierrez *et al.*, 2009; Watanabe *et al.*, 2015). Given the similarity in estimated lifetimes of PCW and SCW CESAs, the large increase in cellulose chain length in SCWs compared with PCWs may instead be dependent on other factors such as the speed of cellulose synthesis, or overall membrane fluidity; however, further experimental work is required to test this hypothesis.

### *Microtubule guidance of CSCs*

CSCs closely follow the tracks of cortical microtubules lying underneath the plasma membrane in both PCW (Paredez *et al.*, 2006; Fujita *et al.*, 2011) and SCW synthesis (Watanabe *et al.*, 2015), supporting the model that cortical microtubules dictate the orientation of cellulose deposition in cell walls (Ledbetter and Porter, 1963). This is highlighted in SCW synthesis, where treatment with the microtubule-depolymerizing drug oryzalin led to the loss of CSC banding patterns at SCW domains (Gardiner *et al.*, 2003; Wightman and Turner, 2008; Watanabe *et al.*, 2015). In PCWs, this microtubule guidance has been shown to be dependent on the cellulose synthase interacting (CSI) proteins CSI1/POM2 and CSI3 (Gu *et al.*, 2010; Bringmann *et al.*, 2012; Li *et al.*, 2012; Lei *et al.*, 2012, 2013). Similar functions have now been demonstrated during SCW synthesis. CSI1/POM2 was enriched in microtubule pull-downs of arabidopsis SCW-producing cell cultures (Derbyshire *et al.*, 2015). Aberrant SCW patterning was then observed in cells where *CSI1/POM2* was knocked down using RNA interference (RNAi) (Derbyshire *et al.*, 2015). Similar patterning defects were recently characterized in native tracheary elements of arabidopsis and rice (*Oryza sativa*) knock-downs (Schneider *et al.*, 2017). This study also showed that CSI1/POM2 co-localizes and co-migrates with SCW CSCs at the plasma membrane. Loss of CSI1/POM2 results in the uncoupling of CSC trajectories from microtubule tracks during early stages of SCW formation, further supporting a role for these proteins in SCW patterning (Schneider *et al.*, 2017).

Although CSI1/POM2 suggests a mechanism for microtubule guidance of CSCs, CSCs may in turn exert force on the underlying cortical microtubules, leading to cross-talk between CSCs and microtubule patterning and dynamics. Indeed, disruption of cellulose synthesis during PCW production with CESA inhibitors, or via mutations, has been shown to alter the cortical microtubule network (Fisher and Cyr, 1998; Paredez *et al.*, 2008). This is highlighted in mutants of the cellulose synthase–microtubule uncoupling (CMU) proteins, where the force of CSC movement along a linear trajectory was able to displace microtubules that they encountered (Liu *et al.*, 2016). CMU proteins bind microtubules *in vitro*, and are hypothesized to anchor the microtubules to the plasma membrane (Liu *et al.*, 2016). The displacement force exerted by CSCs on the underlying cortical microtubules may help explain the observed cross-talk between CSCs and microtubule patterning and movement. Companion of cellulose synthase (CC) has also been shown to link CESAs to microtubules, as fluorescently tagged CC co-localized and moved with CESA particles at the plasma membrane, indicating that CC may be a part of CSCs (Endler *et al.*, 2015). Loss of these proteins decreased CESA delivery to the plasma membrane and CESA velocity during salt stress (Endler *et al.*, 2015). Additionally, loss of CCs severely inhibited microtubule re-formation, while the presence of CCs promoted microtubule polymerization (Endler *et al.*, 2015). The roles of CCs and CMUs have yet to be explored during SCW synthesis, although they have been identified in cells undergoing SCW formation (Derbyshire *et al.*, 2015). Thus, it is reasonable to hypothesize that both sets of proteins play a role in ensuring that CSCs remain within the strict confines of SCW-forming plasma membrane domains, similar to CSI1/POM2. This may be especially important in SCW production given the large density of CSCs present in these domains, which may lead to larger forces on the underlying cortical microtubules. The loss of these proteins might lead to more diffuse SCW domains as the microtubules would no longer restrict CSC movement.

### *Non-CESA proteins involved in cellulose synthesis.*

In addition to microtubule-associated proteins, a number of other proteins have been implicated in cellulose production in SCW synthesis. One such protein, KORRIGAN (KOR), is a membrane-bound endo-(1,4)-β-glucanase that has been linked to control of cellulose crystallinity across plant species (Maloney and Mansfield, 2010; Maloney *et al.*, 2012). In PCWs, loss of KOR or its endoglucanase activity resulted in decreased CSC velocity and defects in microtubule organization (Paredez *et al.*, 2008; Lei *et al.*, 2014) ultimately leading to decreases in cellulose content (Sato *et al.*, 2001; Lane *et al.*, 2001). The importance of KOR in SCW cellulose synthesis is reflected by its identification as one of the first irregular xylem (*irx2*) mutants (Szyjanowicz *et al.*, 2004). Recently it has been shown, through yeast two-hybrid screens, bimolecular fluorescence complementation (BiFC) and live-cell imaging, that in PCWs, KOR directly interacts with CESAs and is a part of CSCs (Mansoori *et al.*, 2014; Vain *et al.*, 2014). However, the exact molecular role of KOR in cellulose synthesis remains to be resolved. This is a common theme among many of the other proteins linked to cellulose synthesis, especially those associated with SCW cellulose synthesis, including Tracheary Element Differentiation-Related6 (TED6) and TED7, transmembrane proteins that may be a part of CSCs in SCWs (Endo *et al.*, 2009; Rejab *et al.*, 2015); COBRA-LIKE4, a lipid anchored protein with a putative cellulose-binding domain (Li *et al.*, 2003; Liu *et al.*, 2013); and CHITINASE-LIKE1(CTL1)/POM1 and CTL2, which can bind to glucan polymers, but lack glucanase activity (Zhang *et al.*, 2004; Sánchez-Rodríguez

*et al.*, 2012). Mutation or loss of any of these genes results in reduced cellulose content and quality within SCWs, making investigation into how each of these gene products contributes to SCW cellulose biosynthesis exciting areas of future study.

## HEMICELLULOSES

When cellulose microfibrils are extruded from the CSC at the plasma membrane into the forming SCW, they interact with hemicelluloses to form a stable network (Simmons *et al.*, 2016). The Golgi-synthesized hemicelluloses make up 10–40 % of the SCW, and are essential for normal growth and development (reviewed in Scheller and Ulvskov, 2010; Rennie and Scheller, 2014; Kumar *et al.*, 2016*a*). The type and quantity of SCW hemicelluloses varies with species and cell type, but in general xylans and mannans are most common (Scheller and Ulvskov, 2010). Xylans of the eudicot SCW are characterized by a β-(1,4)-linked xylose backbone, decorated with side chains of glucuronic acid (glucuronoxylan), while conifer xylans are also substituted with varying amounts of arabinose (Ebringerová, 2005). A recent survey of monocot xylans suggests that non-grass monocots have more eudicot-like glucuronoxylan-containing SCWs, while grasses contain arabinose-substituted SCW xylans (Peña *et al.*, 2016). Mannans are the most abundant hemicellulose in conifer SCWs, and smaller amounts are also found in the walls of dicots and grasses (reviewed in Rodríguez-Gacio *et al.*, 2012). These carbohydrates have a β-(1,4)-linked mannose and glucose backbone, and, in conifers, side chains of galactose are seen. Xylans and mannans are also variously acetylated and/or methylated, a process that is thought to be important for ensuring their solubility and their final conformation (Urbanowicz *et al.*, 2012; Pawar *et al.*, 2013; Rennie and Scheller, 2014). Subsequent deacetylation of xylan was recently shown to be important for proper patterning of rice SCWs (Zhang *et al.*, 2017).

The cell biology of xylan and mannan synthesis and deposition is centred in the Golgi (Fig. 4). The Golgi is characterized by its complex, three-dimensional structure, including the forming *cis*-face that interacts with the ER, the medial Golgi where hemicellulose synthesis is thought to occur, and the *trans*-Golgi cisternae and *trans*-Golgi network (TGN) where secretory vesicles form. Recent research into biosynthesis of SCW hemicelluloses has identified and characterized many of the glycosyltransferases, substrate transporters and other Golgi-resident proteins important for hemicellulose biosynthesis (reviewed in Hao and Mohnen, 2014; Kumar *et al.*, 2016*a*). Similarly, numerous cell biology studies have characterized the vesicle budding, tethering and fusion machinery of the plant endomembrane system, which are necessary for Golgi function (reviewed in Worden *et al.*, 2012; Gendre *et al.*, 2015; Kim and Brandizzi, 2016). However, these two fields have not been well integrated, so it is unclear how glycosyltransferases are co-ordinated to produce SCW hemicelluloses within specific regions of the Golgi, and how the associated trafficking machinery maintains these Golgi-resident proteins. Here, we explore the Golgi as a platform for hemicellulose biosynthesis, and discuss how the complex structure and function of the Golgi can support the massive production of hemicelluloses required for the SCW.

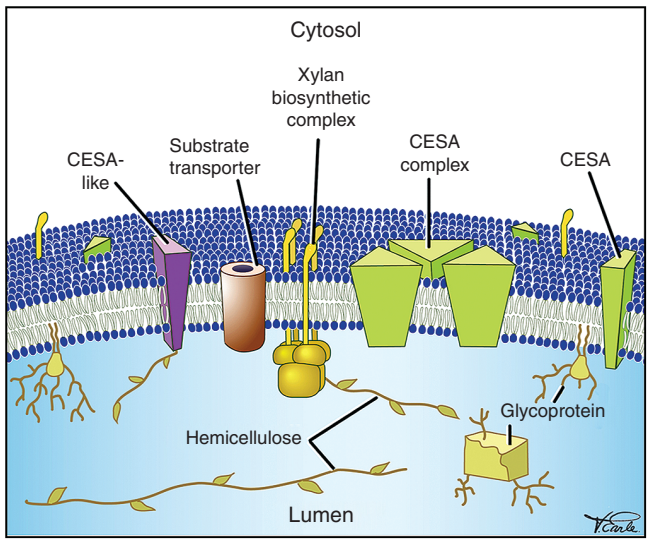


FIG. 4. Cross-section of part of a SCW-producing Golgi cisterna. The Golgi contains resident proteins (e.g. xylan biosynthetic complexes, CESA-like mannan synthase and substrate transporters) and cargo (hemicelluloses such as xylan and mannan, glycoproteins such as laccases, and CESAs), which are modified or produced in the Golgi and secreted to the SCW.

### *Hemicellulose biosynthetic complexes*

During SCW production, the Golgi is remobilized from PCW production to begin assembly of xylans and mannans, and to modify and traffic the large number of proteins required for proper cellulose and lignin deposition, e.g. CESAs and laccases/peroxidases. This requires loading the flattened, membrane-bound cisternae of the Golgi stacks with the many proteins necessary to carry out these functions. Synthesis of xylan alone is thought to require over a dozen proteins including glycosyltransferases, acetyltransferases, methyltransferases, substrate transporters and proteins involved in substrate synthesis (reviewed in Rennie and Scheller, 2014; Kumar *et al.*, 2016*a*). These proteins must then work in concert in the Golgi to enable efficient xylan synthesis.

One way in which cells could encourage efficient hemicellulose production in the Golgi is via the formation of protein complexes. There is growing evidence that complex formation is a key feature of many types of Golgi-resident proteins, including those involved in *N*-glycan processing and mannan and xylan synthesis (reviewed in Oikawa *et al.*, 2013). For example, three sets of proteins have been implicated in synthesis of the xylan backbone in arabidopsis SCWs: IRX9/IRX9L (Lee *et al.*, 2010; Wu *et al.*, 2010), IRX10/IRX10L (Brown *et al.*, 2009; Wu *et al.*, 2009) and IRX14/IRX14L (Keppler and Showalter, 2010). Evidence that xylan biosynthetic proteins can form a complex comes from CoIP and BiFC studies of PCW production of arabinoxylans in wheat (*Triticum aestivum*) and asparagus (*Asparagus officianalis*), demonstrating *in planta* heterodimerization of xylan biosynthetic proteins orthologous to the arabidopsis proteins (Zeng *et al.*, 2010, 2016). Each protein was also shown to homodimerize *in planta*, further increasing the size of the proposed xylan biosynthetic complex to at least six members (Zeng *et al.*, 2016). The formation of the core xylan biosynthetic complex containing IRX9, IRX10 and IRX14 may also be a prerequisite for their Golgi localization,

as transiently expressed asparagus IRX9, IRX10 and IRX14 were retained in the ER unless co-expressed with the other two proteins (Zeng *et al.*, 2016). This may explain why protein–protein interactions were not detected in pairwise combinations of arabidopsis IRX9, IRX10 and IRX14 using a luciferase assay (Lund *et al.*, 2015). Furthermore, because IRX10 lacks a transmembrane domain, it may be maintained in the Golgi via its interactions with IRX9 or IRX14, as has been shown for the mature luminal form of the pectin biosynthetic protein GAUT1 and its partner GAUT7 (Atmodjo *et al.*, 2011).

The different functions of IRX9, IRX10 and IRX14 in a xylan biosynthetic complex have been dissected using site-directed mutagenesis of the arabidopsis (Ren *et al.*, 2014) and asparagus proteins (Zeng *et al.*, 2016). Mutation of the proposed glycosyltransferase catalytic and UDP-xylose substrate-binding domains of IRX9/IRX9L did not impede complementation of the mutant phenotype or xylosyltransferase activity of the biosynthetic complex, indicating that their function may be structural rather than enzymatic (Ren *et al.*, 2014; Zeng *et al.*, 2016). Similarly, IRX14 has been proposed to be important for substrate binding (Zeng *et al.*, 2016) or priming of xylan synthesis (Ren *et al.*, 2014), as its function was impaired when the substrate-binding site was mutated. Finally, catalytic function has been ascribed to IRX10/IRX10L, as heterologously expressed Arabidopsis IRX10L has been shown to have xylan xylosyltransferase activity *in vitro* (Urbanowicz *et al.*, 2014). This function is likely to be conserved among IRX10 orthologues and paralogues, as xylosyltransferase activity has also been observed for IRX10 from psyllium (*Plantago ovata*) and *Physcomitrella patens* (Jensen *et al.*, 2014). Proteins involved in decoration of the xylan backbone may also be incorporated into the protein complex, as a PCW xylan biosynthetic complex isolated from wheat also showed arabinosyltransferase and glucuronosyltransferase activity necessary for side chain addition (Zeng *et al.*, 2010). Furthermore, because the UDP-xylose substrate for xylan backbone synthesis is now believed to be synthesized in the cytosol (Kuang *et al.*, 2016; Zhong *et al.*, 2016), the Golgi-localized UDP-xylose transporters, especially UXT1, are hypothesized to be similarly associated with the xylan biosynthetic complex to ensure adequate substrate availability (Ebert *et al.*, 2015).

### *Models of Golgi processing and their implications for hemicellulose biosynthesis*

Despite the evidence for hemicellulose biosynthetic complex formation in the Golgi, we still know little about how these proteins are arranged in the cisternae. This is important because the Golgi is the platform on which hemicellulose biosynthesis occurs and, as such, is as critical to hemicellulose synthesis as the plasma membrane is to cellulose biosynthesis. As materials move through the Golgi stack, there are changes in pH, cisternal structure, and lipid, polysaccharide and protein composition (reviewed in Day *et al.*, 2013; Ito *et al.*, 2014). Because of this changing microenvironment across the Golgi, the localization of hemicellulose biosynthetic enzymes in the Golgi stack could affect their activity, what proteins they can interact with, the availability of their substrates, how they maintain their position in the Golgi and how their products transit the Golgi.

A wide variety of evidence suggests that Golgi cisternae mature over time; *cis*-cisternae evolve into medial- and *trans*-cisternae with differing compositions of resident proteins and gradual modification and accumulation of cargo (reviewed in Glick and Luini, 2011). In this traditional cisternal maturation model, hemicellulose biosynthetic proteins are predicted to maintain their position in the stack of maturing cisternae via recycling in coat protein I- (COPI) coated vesicles budding from the cisternal margins. At the same time, the hemicellulose products are predicted to accumulate in swollen cisternal margins, and then be released in secretory vesicles budding at the *trans* face of the Golgi. However, the processes partitioning hemicellulose biosynthetic proteins from their products during cisternal maturation are not well understood. Furthermore, a few studies suggest that Golgi processing is not so straightforward. In addition to its role in vesicle formation, COPI has now been shown to facilitate formation of tubules containing anterograde cargo in mammalian cell culture (Yang *et al.*, 2011). These tubules were then shown to be involved in either anterograde or retrograde intra-Golgi trafficking, depending on the activity of a small GTPase (Park *et al.*, 2015). Much of the machinery governing Golgi structure and function, including vesicle formation and fusion proteins, are highly conserved among eukaryotes (Klute *et al.*, 2011). The diverse functions of COPI, in formation of vesicles and tubules, and in anterograde and retrograde trafficking, may be similarly conserved among yeast, animals and plants. This raises questions about the precise role of COPI in mediating trafficking of hemicellulose biosynthetic proteins and sequestering them from hemicellulose cargo.

There is a growing body of evidence showing that the formation of protein complexes can itself affect the localization of resident proteins in the Golgi stack, which has interesting implications for the arrangement of SCW hemicellulose biosynthetic complexes in the Golgi. Earlier models, based on freeze-fracture/TEM and immuno-gold labelling/TEM, predicted that glycosyltransferases are arranged in protein arrays in the compressed cisternal centres, and that their finished cargo accumulate in the swollen margins (Staehelin *et al.*, 1990). This sequestration of polysaccharide cargo may depend on its physical properties such as size, solubility and conformation. More recent cryo-TEM tomography of *Chlamydomonas* Golgi corroborates the presence of protein arrays bridging the lumen in the centres of *trans*-cisternae (Engel *et al.*, 2015), but there is still no direct evidence that these structures contain glycosyltransferases. Furthermore, live-cell imaging contradicts this model, as many hemicellulose biosynthetic enzymes, including IRX9L (Zhang *et al.*, 2016), have a characteristic ‘ring-shaped’ Golgi localization, suggesting that these proteins may instead be depleted in cisternal centres. Additionally, in mammalian cells, inducible oligomerization of an engineered Golgi-resident protein was found to shift the localization of that protein reversibly toward more *trans*-cisternae and cisternal centres (Rizzo *et al.*, 2013). The formation of large hemicellulose biosynthetic complexes may similarly affect their localization and function in the plant Golgi.

The division of the Golgi into discrete cisternae has long been hypothesized as a mechanism of spatially segregating sequential processing stages, and hence different glycosyltranferases and processing enzymes, across the Golgi stacks. While the strongest evidence for this ‘assembly-line’ model of

Golgi processing comes from *N*-glycan glycoprotein literature (reviewed in Schoberer and Strasser, 2011), this sequential glycosylation model has been extrapolated to PCW polysaccharide biosynthesis (Chevalier *et al.*, 2010). In these models, carbohydrate backbone synthesis is often proposed to occur earlier in the Golgi, followed by addition of side chains, methylation and acetylation. If the SCW hemicellulose backbone biosynthetic complexes also contain the proteins required for carrying out such modifications, then it would suggest that this kind of stack sub-compartmentalization is not occurring. However, analysis of xylans in various xylan biosynthetic mutants suggests that the methylation rate of glucuronic acid residues is independent of the rate of xylan synthesis, which is consistent with a post-backbone synthesis methylation model (Zhong *et al.*, 2005; Peña *et al.*, 2007; Kuang *et al.*, 2016). Furthermore, many SCW xylans have a conserved oligosaccharide at their reducing end (Peña *et al.*, 2016), which has been hypothesized to be either a primer for consecutive xylan synthesis or a terminator of synthesis, transferred *en bloc* to the completed xylan backbone (York and O'Neill, 2008). In either model, different steps in xylan synthesis are proposed to occur sequentially. Xylans also have alternating 'major' and 'minor' domains with differing patterns of glucuronic acid substitution (Bromley *et al.*, 2013). These different domains may reflect variation in the rate of substitution on a consecutively synthesized xylan backbone, but they could also be synthesized independently and then assembled into a single strand later in the Golgi. Ultimately, it is reasonable to hypothesize that some measure of spatial segregation occurs across Golgi cisternae during xylan production, but this model will have to be reconciled with the growing recognition of the importance of biosynthetic complexes, at least for backbone synthesis.

### *Simultaneous synthesis of SCW hemicellulose and protein cargos*

Production of the large volume of hemicelluloses required for SCW deposition requires the co-ordinated action of the hundreds of Golgi stacks making up the cell's Golgi apparatus. The number of Golgi stacks is predicted to increase with both cell size and the demand for Golgi cargo. For example, during seed coat development in arabidopsis, or in rapidly growing tobacco BY-2 cells, an increase in the number of Golgi stacks coincides with an increase in Golgi residents and cargo necessary for extensive production and secretion of cell wall materials (Young *et al.*, 2008; Toyooka *et al.*, 2014). The onset of SCW production may therefore coincide with a similar increase in the number of individual Golgi stacks in these cells.

At any given time during SCW production, the Golgi apparatus is synthesizing several types of polysaccharides, carrying out *N*- and *O*-glycan processing, and processing the numerous and varied proteins destined for the vacuole, plasma membrane or cell wall. This raises the question of whether each Golgi stack in the cell carries out these functions simultaneously, or if distinct sub-populations of Golgi bodies specialize in different kinds of processing. TEM immunolabelling experiments have shown that Golgi in epidermal cells of arabidopsis seeds and suspension-cultured cells of sycamore maple can produce pectin and xyloglucan simultaneously (Zhang and Staehelin, 1992; Young *et al.*, 2008), suggesting that Golgi do not specialize in one type of polysaccharide synthesis. If this holds true in SCW biosynthesis, we can expect that xylans and mannans, and possibly glycoproteins, are made simultaneously in each Golgi stack.

## POST-GOLGI TRAFFICKING OF SCW CARGO

### *Diverse populations of post-Golgi vesicles in SCW biosynthesis*

At the *trans*-face of the Golgi, hemicelluloses and secreted proteins are sequestered from the Golgi-resident proteins, and packaged into secretory vesicles for delivery. This process is thought to occur as the curved, and collapsing *trans*-Golgi cisterna matures into a TGN composed of a highly interconnected cluster of secretory and clathrin-coated vesicles (Kang *et al.*, 2011). In developing pine tracheids, the TGN and associated vesicles were found to contain mannans being secreted to the SCW (Samuels *et al.*, 2002). At the TGN, diverse kinds of cargo must be packaged into vesicles for secretion to the SCW, and it is currently unclear whether secreted polysaccharide and protein cargo are trafficked in different populations of vesicles. If they are trafficked together, glycosylated SCW proteins, such as the laccases and peroxidases required for lignin polymerization, could physically interact with the polysaccharides before they are secreted, and thereby affect SCW assembly. In mutants of the post-Golgi trafficking protein ECHIDNA, PCW polysaccharide cargo is misdirected to the vacuole while some protein cargo is not, indicating that there are different mechanisms for targeting these different types of cargo from the TGN to the plasma membrane (Gendre *et al.*, 2013; McFarlane *et al.*, 2013). Whether these mechanisms include segregation into independent populations of secretory vesicles remains to be determined. The possibility of cargo segregation at the Golgi is supported by a recent study in mucilage-producing root border cells of alfalfa (*Medicago sativa*) that identified two populations of vesicles, with distinct polysaccharide cargos, budding from different locations in the Golgi stack (Wang *et al.*, 2017). The TGN also serves a dual function in the cell, as a sorting hub for both exocytosis and endocytosis in either a Golgi-associated or a Golgi-free form (Viotti *et al.*, 2010; Kang *et al.*, 2011). From the TGN, endocytic materials can be re-secreted to the plasma membrane or travel to the vacuole for degradation, via multivesicular bodies (reviewed in Uemura, 2016). The importance of endocytosis in SCW deposition is often underemphasized, but it has an important function in the recycling of lipids and trafficking machinery from the plasma membrane to the TGN, thereby allowing continued secretion of hemicellulose and proteins.

One important but enigmatic population of post-Golgi compartments are the small CESA compartments (SmaCCs), which dynamically interact with the Golgi and plasma membrane during SCW biosynthesis (Watanabe *et al.*, 2015). SmaCCs are a diverse population of compartments, as only a sub-set of SmaCCs co-localized with the TGN marker VHAa-a1 (Crowell *et al.*, 2009). They have been shown to deliver CSCs to the plasma membrane in both PCW and SCW formation (Gutierrez *et al.*, 2009; Watanabe *et al.*, 2015), and experiments with PCW CESAs have also implicated them in CESA endocytosis and recycling (Crowell *et al.*, 2009; Gutierrez *et al.*, 2009).

CESAs in the plasma membrane are known to be reversibly internalized under osmotic stress and upon treatment with drugs such as isoxaben (Crowell *et al.*, 2009; Fujimoto *et al.*, 2015). The endocytic nature of SmaCCs is strongly supported by data showing that CESA internalization under stress coincides with accumulation of a population of SmaCCs tethered to microtubules, termed microtubule-associated cellulose synthase compartments (MASCs) (Crowell *et al.*, 2009). PCW CESA signal near the plasma membrane co-localizes with clathrin light chains (CLCs), implying that CESAs are endocytosed via a clathrin-dependent pathway (Miart *et al.*, 2014). Together, these data have led to the hypothesis that SmaCCs are involved in routine recycling of CESAs from the plasma membrane to the TGN before re-secretion (Bashline *et al.*, 2013). Interestingly, CESA endocytosis does not co-localize with FM 4–64, a standard endocytic marker (Gutierrez *et al.*, 2009), which may reflect exclusion of this dye from the lipids around an endocytosing CSC.

The importance of endocytosis in CESA function is further demonstrated by data showing that loss of the clathrin adaptor proteins, μ2/AP2M or TWD-40–2, results in an increase in CESA signal at the plasma membrane (Bashline *et al.*, 2013, 2015). The loss of both adaptor proteins leads to decreases in CSC velocities and deficiencies in cellulose content (Bashline *et al.*, 2015). CESA endocytosis was also found to be important during SCW production in rice (Xiong *et al.*, 2010). A dynamin-related protein implicated in clathrin-mediated endocytosis, DRP2B, had aberrant SCW structures when overexpressed or lost (Xiong *et al.*, 2010). The function of CESA endocytosis is not currently known, but, given the decrease in cellulose quality or quantity in mutants deficient in CESA internalization, endocytosis may be a quality control mechanism ensuring degradation of non-functional CESAs, while functional proteins are integrated into new CSCs for re-secretion (Bashline *et al.*, 2013, 2015). The mechanism by which CESAs are targeted for endocytosis has not been elucidated, as it occurs infrequently under normal conditions (Bashline *et al.*, 2013), but clues may be provided by studying the transition from PCW to SCW synthesis (Z. Li *et al.*, 2016), when PCW CESAs may be internalized in bulk.

### *Targeting of secretory vesicles to SCW domains*

After secretory vesicles form, they must be targeted to their site of exocytosis at the forming SCW. Secretory vesicles are targeted to cortical microtubule arrays that line regions of the plasma membrane where the SCW is being actively deposited (Oda *et al.*, 2015; Watanabe *et al.*, 2015). This is highlighted in arabidopsis metaxylem cell cultures, where microtubule patterning was shown to be established and maintained by recruitment of the microtubule-depolymerizing protein kinesin-13A to specific plasma membrane regions (Oda and Fukuda, 2012, 2013). This important patterning function of microtubules was leveraged to identify and characterize other players in SCW secretion via a microtubule pull-down and proteomics analysis in arabidopsis xylem cell culture (Derbyshire *et al.*, 2015). Among the 600+ identified proteins, several of the microtubule-associated proteins, including MAP65 and AIR9, displayed altered SCW patterning when knocked down or overexpressed.

In plant cells, actin microfilaments are responsible for myosin-mediated cytoplasmic streaming of cellular contents, including the Golgi and post-Golgi vesicles (reviewed in Tominaga and Ito, 2015). Live-cell imaging in PCW-producing cells showed that CESA-containing vesicles travel along endoplasmic actin microfilaments throughout the cell (Sampathkumar *et al.*, 2013). Actin disruption by drug treatment or actin mutants resulted in an uneven accumulation of CESAs at the plasma membrane near Golgi stacks (Crowell *et al.*, 2009; Gutierrez *et al.*, 2009; Sampathkumar *et al.*, 2013), indicating that while CESAs were successfully delivered to the plasma membrane in the absence of actin, their distribution was altered. Actin has also been implicated in proper SCW patterning, as disruption of actin polymerization resulted in aberrant microtubule banding and SCW patterning in *Zinnia* xylem cell cultures (Kobayashi *et al.*, 1988), and loss of CESA banding in native arabidopsis root tracheary elements (Wightman and Turner, 2008). This phenotype may be a result of altered pausing of Golgi in regions close to SCWs, as paused Golgi go on to deliver CSCs to the plasma membrane in cells producing both PCWs and SCWs (Crowell *et al.*, 2009; Gutierrez *et al.*, 2009; Sampathkumar *et al.*, 2013; Watanabe *et al.*, 2015; Schneider *et al.*, 2017). However, Golgi pausing at SCW domains continued when the microtubules lining them were depolymerized, implicating actin in the process of Golgi pausing (Wightman and Turner, 2008; Schneider *et al.*, 2017).

Secretory vesicles must also be tethered to their target membranes prior to fusion. Tethering of vesicles to the plasma membrane in eukaryotes can be facilitated by the octomeric exocyst complex, which interacts with proteins on vesicles and their target membranes (reviewed in Synek *et al.*, 2014). Two exocyst components, EXO70A1 and EXO84B, localize to SCW domains, and mutants in *exo70A1* and *exo84B* have aberrant SCW patterning, with an accumulation of large vesicles in developing tracheary elements (Li *et al.*, 2013; Vukašinović *et al.*, 2017). While CESA banding at SCW domains was disrupted in *exo70A1* and *exo84B* mutants, patterned secretion of laccases did not appear to be affected (Vukašinović *et al.*, 2017), suggesting that luminal secreted proteins may traffic in different vesicles compared with the membrane-bound CESAs. In developing xylem, a population of post-Golgi vesicles containing the Vesicle Tethering1 (VETH) and conserved oligomeric Golgi (COG) protein complex are associated with the microtubules lining SCW domains (Oda *et al.*, 2015). Furthermore, fluorescence resonance energy transfer (FRET) microscopy showed that members of the exocyst complex interact with the VETH–COG complex (Vukašinović *et al.*, 2017). However, VETH-labelled compartments track the plus-ends of microtubules, and are therefore not fully compatible with certain populations of SmaCCs/MASCs (Oda *et al.*, 2015), which are associated with both plus- and minus-ends (Gutierrez *et al.*, 2009), again suggesting the presence of multiple populations of SmaCC vesicles.

Additionally, proper vesicle targeting to the plasma membrane is dependent on the composition of phosphatidylinositol phosphate (PIP) lipids on the different organelle membranes (reviewed in Krishnamoorthy *et al.*, 2014; Heilmann and Heilmann, 2015). Differentially phosphorylated PIPs have important roles in establishing membrane identity and allowing docking of distinct kinds of proteins. The phosphorylation

state of PIPs is regulated by various kinases (PIPKs) and phosphatases (PTases). In arabidopsis roots, the PIP kinase PIP4K, and other endomembrane machinery, is associated with budding secretory vesicles containing PCW hemicelluloses (Kang *et al.*, 2011). The PIP kinase PI3K, which produces PI3P lipids, has been shown to be essential for proper delivery of PCW CESAs to the plasma membrane (Fujimoto *et al.*, 2015). PI-binding proteins may have a conserved function in SCW-producing cells, helping to establish the membrane identity of secretory vesicles and their target membranes, allowing for proper budding and tethering of vesicles destined for the SCW. This is supported by a study showing reduced SCW thickness in arabidopsis fibre cells in a PIP phosphatase mutant (*fra3*) (Zhong *et al.*, 2004).

In the post-Golgi trafficking of SCW hemicelluloses, CSCs and glycoproteins, all the components necessary to build the SCW are delivered to the plasma membrane in a co-ordinated manner. The cytoskeleton directs this delivery to produce the spiral, annular or pitted patterns of the SCW in different cell types. This process creates the polysaccharide scaffold of the SCW, into which the lignin polymer is deposited.

## LIGNIN

Unlike the other components of SCWs, which are polysaccharide in nature, lignin is a heteropolymer of 4-hydroxyphenylpropanoids derived from the amino acid phenylalanine. Typically, lignin forms when the three monolignols (*p*-coumaryl alcohol, coniferyl alcohol and sinapyl alcohol) are oxidized to monolignol radicals in the SCW, and undergo combinatorial coupling into H-, G- and S-lignin, respectively. Lignification is the last step of SCW biosynthesis, establishing the final, functionally mature wall that supports the plant and persists after vascular cells, such as vessels, undergo programmed cell death. With lignin comprising about 30 % of woody cell wall biomass (Campbell and Sederoff, 1996), this aromatic polymer represents an important SCW component. Our understanding of lignin has advanced recently due to both fundamental research in molecular genetics, biochemistry and genomics, and research motivated by bioenergy applications (reviewed by Bonawitz and Chapple, 2010; Vanholme *et al.*, 2010; Mottiar *et al.*, 2016). While this has revealed many aspects of the biosynthetic machinery associated with the general phenylpropanoid pathway and monolignol biosynthesis, we have only recently been able to put monolignol production, monolignol export and the heterogeneity of extracellular polymerization of lignin into the context of diverse lignifying plant cells in complex tissues.

### *Monolignol biosynthesis*

Monolignols are made in the cytosol via the general phenylpropanoid and monolignol biosynthetic pathways, as demonstrated by many studies documenting loss-of-function mutants and plants with knock-downs of pathway genes in arabidopsis, poplar and alfalfa (reviewed by Bonawitz and Chapple, 2010; Dixon *et al.*, 2014). Loss of monolignol biosynthetic genes leads to complex metabolic and transcriptomic phenotypes, which were revealed with a systems biology approach (Vanholme *et al.*, 2012). In arabidopsis, mutant lines with reduced lignin levels had upregulation of the upstream shikimate and phenylpropanoid pathways, while the mutants with similar lignin levels but altered composition had decreases in shikimate and phenylpropanoid gene expression (Vanholme *et al.*, 2012). One important consistent feature of studies of mutant plants with altered expression of monolignol biosynthetic genes is the plasticity of the lignin polymer to accept non-canonical monomeric units (Bonawitz and Chapple, 2010; Dixon *et al.*, 2014; Mottiar *et al.*, 2016). The lignin polymer commonly has a composition rich in S and G monolignols. However, this composition is flexible, as variability is seen not only in lignin biosynthetic mutants, but also in natural lignins from diverse plant species which contain atypical monolignols (Chen *et al.*, 2013; Zhao, 2016). In addition, a common phenotype of monolignol biosynthetic mutants is accumulation of phenolic glucosides of metabolites upstream of the genetic lesion, or of biosynthetically related metabolites (Morreel *et al.*, 2004; Anderson and Chapple, 2014; Dixon *et al.*, 2014). These studies not only identify the genes responsible for monolignol biosynthesis, but they also demonstrate the complex metabolic feedback networks governing phenylpropanoid and monolignol metabolism.

The expression of monolignol biosynthetic genes in lignifying cells has been well documented (Barros *et al.*, 2015). However, as many xylem cells continue to lignify after programmed cell death, it has been hypothesized that in addition to the lignifying cell itself, 'good neighbour' cells, living parenchyma in the xylem adjacent to the lignifying cells, may contribute monolignols to the shared cell wall (Hosokawa *et al.*, 2001; Pesquet *et al.*, 2013). In lignifying arabidopsis stems, a SCW CESA promoter was used to drive monolignol knockdown using microRNA specifically in cells developing thickened SCW, so any resulting lignification was the result of good neighbours (Smith *et al.*, 2013). Interestingly, vascular bundles continued to lignify, suggesting that xylem parenchyma cells were good neighbours, an interpretation that was verified by knocking down monolignol biosynthesis using a xylem–parenchyma-specific promoter (Smith *et al.*, 2017). In contrast to the vascular bundles, when monolignol biosynthesis was knocked down in the sclerenchymous fibres, their lignification was strongly adversely affected, indicating that the interfascicular fibres of the arabidopsis stem are cell-autonomous for lignification (Smith *et al.*, 2013, 2017). These experiments indicate that lignification of a tissue is the result of a community of cells, some of which produce their own monolignols, and some of which accept or donate monolignols.

Modification of monolignol metabolism can have a strong impact on the growth of a plant, as seen in the lignin modification-induced dwarfism of a number of arabidopsis mutants such as *c3'h*, *hct*, *ccr1* and *cse* (Bonawitz and Chapple, 2010; Vanholme *et al.*, 2012). While at first glance, this is attributed to the irregular xylem phenotype due to weakened SCW, it is likely that soluble phenolic signalling compounds also play important roles. For example, lignin modification-induced dwarfism of *c3'h/ref8* can be relieved by loss of function of specific components of the conserved eukaryotic transcriptional co-regulatory complex Mediator (MED) (Bonawitz *et al.*, 2012, 2014). Plants with triple *med5a med5b c3'h* mutations had wild-type growth and lignin levels, although the quality of the lignin was shifted

from the typical S/G of the wild type to almost entirely H-lignin (Bonawitz *et al.*, 2014). Analysis of loss- and gain-of-function *med5a med5b* mutants, as well as analysis of the soluble phenolic profiles of *fah1/f5h* mutants point to a role for MED5a/b as a repressor of phenylpropanoid metabolism (Bonawitz *et al.*, 2012; Anderson *et al.*, 2015). Additional MED-independent mechanisms must operate since the *med5a med5b* mutant background does not rescue all lignin modification-induced dwarfism mutants, e.g. *c4h* (Bonawitz *et al.*, 2014). Restoring lignin to a sub-set of cells, as in the good neighbour experiments above (Smith *et al.*, 2013), or in vessel-specific rescue of lignin modification-induced dwarfism mutants, is also sufficient to restore wild-type growth despite the overall lignin reductions in the whole plant (Yang *et al.*, 2013; Vargas *et al.*, 2016). The relationships between plant growth and developmental lignification of SCWs are just emerging, and these data suggest that biomass loss is not an inevitable consequence of a plant with lower lignin levels. From a bioenergy perspective, tissue-specific changes in lignification, with considerations of vessel integrity and lodging, are likely to be preferable to constitutive knock-down of lignin components.

### *Monolignol export from cells*

The monolignol biosynthetic reactions occur within the cytosol, or in close proximity to the ER, of monolignol-producing cells (Schuetz *et al.*, 2014; Barros *et al.*, 2015). The mechanism of monolignol export from the site of synthesis to the region of the cell wall in which the monolignols become polymerized remains unclear. While in conceptual overviews, lignification is usually simply depicted as the polymerization of three canonical monolignols, there are possible roles for monolignol glucosides (Le Roy *et al.*, 2016) and oligolignols (Morreel *et al.*, 2004; Huis *et al.*, 2012) in the lignification process. This may depend on the taxa, lignifying tissue and cell type. For example, in gymnosperms, but not angiosperms, large amounts of coniferin (the β-glucosyl derivative of coniferyl alcohol) are detected during active lignification (Savidge, 1989). This correlation led to the view that coniferin is the precursor for lignin formation in gymnosperms (Terashima *et al.*, 2016). Coniferin accumulating in vacuoles of lignifying tracheids (Tsuyama and Takabe, 2014) could be released upon programmed cell death to participate in the final stages of lignification following β-glucosidase cleavage of the glucose, and coniferyl alcohol radical formation by laccases/peroxidases. However, autoradiography of developing pine tracheids showed phenylpropanoids rapidly incorporated into cell walls while the cells were still living, without strong labelling of the coniferin pool in the vacuole (Kaneda *et al.*, 2008). This may indicate that both coniferyl alcohol and coniferin can be incorporated into gymnosperm lignin, as suggested by feeding experiments (Tsuji *et al.*, 2004). Earlier in lignification, coniferyl alcohol could be exported to the cell wall, then the vacuolar coniferin pool could be released at the time of programmed cell death. This model is supported by high-resolution mapping of coniferin in developing tracheids of gingko wood, using cryo-scanning electron microscopy (SEM) and time of flight-secondary ion mass spectrometry, where tracheids have large vacuolar reserves of coniferin up to the point of programmed cell death (Aoki *et al.*, 2016). In contrast, in angiosperms, monolignol glucosides do not accumulate, and several lines of evidence suggest that they do not participate in lignification (Le Roy *et al.*, 2016). An interesting observation that arises out of metabolite profiling of plant tissues actively forming lignin is that there are not large pools of intermediates in the monolignol pathway, or the monolignols themselves, in the cells, although oligolignols are detected in the extracellular environment (Chen *et al.*, 2003; Morreel *et al.*, 2004; Laitinen *et al.*, 2017). In lignifying arabidopsis stems, targeted metabolomics reported coniferyl alcohol levels at 3 nmol $g^{-1}$ f. wt, and sinapyl alcohol levels near 23 nmol (Jaini *et al.*, 2017). With lignin levels in these stems at about 20 % of the dry weight, it is clear that the soluble precursors of lignin are rapidly assimilated into the polymer. The scant pools and rapid incorporation of precursors suggests that there are efficient export mechanisms for these components.

So how do monolignols get from inside the lignifying cell, or a 'good neighbour' cell, and out into the developing SCW? Previously, a model of vesicle-mediated monolignol export was suggested based on autoradiography of chemically fixed samples prepared for TEM (Pickett-Heaps 1968). However, studies with cryo-fixed samples do not support the model that monolignols are secreted via the endomembrane system (Kaneda *et al.*, 2008; Smith *et al.*, 2013). The small size of monolignols, and their demonstrated ability to partition into the membrane of synthetic lipid disks, supports the idea that monolignols could instead exit the cell by passive diffusion (Boija and Johansson, 2006; Boija *et al.*, 2007). In this model, monomer export could be driven by the concentration gradient between the cytosol, where monolignols are being actively synthesized, and the cell wall matrix, where they rapidly polymerize into lignin. The rate of diffusion of the monolignols across the plasma membrane would have to be very high to account for the rapid and extensive lignification occurring in the maturing SCW. However, only low levels of monolignol diffusion across the membrane of plasma membrane vesicles have been reported (Miao and Liu, 2010). Perhaps this is expected, since the *in vitro* conditions of isolated plasma membrane vesicles that were tested did not include a lignin polymerization system, so there would not have been a removal of monomers from the system and therefore no force driving the unidirectional movement of monolignols.

Another, not mutually exclusive, model for monolignol export proposes that monolignol export to the cell wall occurs via plasma membrane-localized transporters such as ATP-binding cassette (ABC) transporters (Li and Chapple, 2010; Miao and Liu, 2010; Kaneda *et al.*, 2011; Alejandro *et al.*, 2012). Transport of coniferyl alcohol monolignols into plasma membrane-enriched vesicles was not sensitive to disruption of transmembrane proton gradients, but treatment with chemicals known to act as ABC transporter inhibitors, such as vanadate or nifedipine, reduced monolignol accumulation in these vesicles (Miao and Liu, 2010). Interestingly, monolignol-glucosides were not transported in plasma membrane-enriched vesicles, but they were taken up by vacuole-enriched vesicles in an ATP-dependent manner (Miao and Liu, 2010). In addition, $H^+$/coniferin antiport activity was demonstrated in vesicles prepared from endomembranes of hybrid poplar and Japanese cypress secondary xylem tissue (Tsuyama *et al.*, 2013). While these studies implicate an

ATPase-dependent monolignol transport activity, characterization of candidate transporters has been elusive.

A set of candidate monolignol export ABC transporters was previously identified based on their co-expression with phenylpropanoid biosynthesis genes in developing arabidopsis inflorescence stems (Ehlting *et al.*, 2005). However, no lignin-related phenotypes have been observed in the knockout mutants of these transporters (*abcb11*, *abcb14*, *abcb15*, *abcg29* and *abcg33*) (Kaneda *et al.*, 2011). Further characterization of ABCG29 demonstrated that it is a plasma membrane-localized protein, and expressed in endodermal cells and vascular tissue, the primary locations of lignification in the root (Alejandro *et al.*, 2012). Assays in yeast microsomes showed that this protein was capable of transporting *p*-coumaryl alcohol, but did not show transport activity for coniferyl alcohol or sinapyl alcohol. Knock-out mutations in the ABCG29 gene resulted in a slight root lignin phenotype (Alejandro *et al.*, 2012). Together these data suggest that ABCG29 may be a candidate monolignol exporter for *p*-coumaryl alcohol units in roots. However, since most angiosperm lignin has only small amounts of H-lignin, and therefore a low requirement for *p*-coumaryl alcohol transport, further studies are required to find other transporters capable of efficiently exporting coniferyl alcohol and sinapyl alcohol.

### *Monolignol polymerization in the SCW*

Lignification depends on the oxidative enzymes that will activate the monomers for combinatorial coupling into lignin in the cell wall. Both laccases (Berthet *et al.*, 2011; Zhao *et al.*, 2013) and peroxidases (Shigeto *et al.*, 2015) have been shown to contribute to lignification in different cell types. It has been difficult to pinpoint functions of peroxidase gene products, as they are expressed, often redundantly, in a wide variety of cell types, organs and developmental stages, and are found in large multigene families, e.g. 73 peroxidase genes are encoded in the arabidopsis genome (Shigeto and Tsutsumi, 2016). Arabidopsis mutant phenotypes have been modest, but measurable changes have been found in lignin content in the lignified inflorescence stem (Herrero *et al.*, 2013; Fernández-Pérez *et al.*, 2015*b*; Shigeto *et al.*, 2015). Interestingly, both PRX52 and PRX72 have phenotypes in the interfascicular fibres, but not in the vessels (Fernández-Pérez *et al.*, 2015*a*, *b*), which is consistent with transcriptomic data showing relatively low peroxidase gene expression, compared with laccase expression, in developing vessels (Yamaguchi *et al.*, 2011). Cell-specific knock-down of the arabidopsis *PEROXIDASE64* (*PRX64*) in the Casparian strip of the root endodermis led to inhibition of lignin deposition (Lee *et al.*, 2013). Furthermore, inhibition of peroxidase activity by potassium iodide scavenging of free hydrogen peroxide prevented lignification in the endodermis of arabidopsis roots (Lee *et al.*, 2013), and in the cell cultures of spruce (Laitinen *et al.*, 2017). In addition to demonstrating the essential role of peroxidases in oxidizing monolignols during lignification in the spruce model system, detailed metabolomic and transcriptomic characterization of lignifying and lignin-inhibited cultures revealed that the lignifying cells were dealing with substantial oxidative stress. This study, and similar work in arabidopsis (Dima *et al.*, 2015) and poplar (Niculaes *et al.*, 2014), suggests that monolignol radicals are formed in the oxidative environment of the cytoplasm as well as the cell wall, resulting in a complex pool of dimers and oligolignols that the cell must metabolize. Both glucosylation, with sequestration to the vacuole, and export are hypothesized responses to generation of intracellular oxidation products. Together, these data strongly support roles for peroxidases in lignification; the challenge is to elucidate when and where peroxidases act in development.

Our current paradigm of monolignol radical formation and cross-linking of the lignin polymer arose from the early demonstration that incubation of fungal laccases with monolignols *in vitro* leads to polymer formation (Freudenberg, 1965). Correlation analysis of genes co-expressed with known SCW genes in arabidopsis led to the identification of LAC4/IRX12 (Brown *et al.*, 2005). In addition, *lac4 lac17* mutants were subsequently characterized with additive reduced lignin phenotypes (Berthet *et al.*, 2011). In *Brachypodium*, loss of function of LAC5 led to reduced lignin, particularly in the interfascicular fibres (Wang *et al.*, 2015). The role of laccases was dramatically demonstrated in arabidopsis *lac4 lac11 lac17* triple mutants, that had a severe dwarf phenotype and barely detectable lignin (Zhao *et al.*, 2013). This work indicated that laccases are non-redundant with peroxidases, and they clearly have a role to play in lignification, at least in arabidopsis. Laccase loss-of-function double mutants, *lac4 lac17*, have severely impaired monolignol incorporation into the spiral SCWs of developing protoxylem tracheary elements (Schuetz *et al.*, 2014). When expressed using native promoters, fluorescently tagged LAC4 and LAC17 were localized exclusively to these SCW domains, and not in the PCW, and when LAC4 was overexpressed with a strong constitutive promoter, it could trigger the deposition of exogenously added monolignols into polymer in the PCW (Schuetz *et al.*, 2014). The strict localization of the laccases in SCW domains, and their requirement for lignification of protoxylem tracheary elements, highlights the role of laccases in determining the patterning of lignification in these cells. All of these studies demonstrate the importance of the laccase and peroxidase oxidative enzymes in lignification processes in different cell types and developmental stages.

As described above, these glycoproteins must traffic from the ER through the Golgi, where they are glycosylated, and be secreted to SCW domains. In essence, the living protoplast produces and secretes the components necessary to direct the deposition of the lignin polymer remotely in the extracellular matrix. Lignification begins while the polysaccharide cell wall layers are still being deposited, prior to programmed cell death (Terashima and Fukushima, 1988; Smith *et al.*, 2013). This means that the oxidative enzymes will be secreted at the same time as hemicelluloses and CSCs. Interestingly, correlation analyses of signals from both hemicelluloses, labelled with specific antibodies, and lignin autofluorescence, in mature radiata pine wood demonstrated that the strongest lignin signals were in the S1 and S3 layers and were associated with xylan hemicelluloses, which are a relatively minor component of the normal gymnosperm wood. Conversely, galactoglucomannan, the major conifer hemicellulose, dominated the S2 layer and was associated with relatively lower lignin (Donaldson and Knox, 2012). Similar observations were made in another gymnosperm, *Cryptomeria japonica* (Kim *et al.*,

2010; 2011). Assuming that the fluorescence intensity reflects greater lignin levels, these data imply that several developmental shifts must occur during tracheid development, where co-ordinated production and secretion of both different hemicelluloses and varying oxidative enzymes could lead to the observed heterogeneity of S1, S2 and S3 layers of the SCW. Furthermore, in many cell types, such as tracheary elements that rapidly undergo programmed cell death, lignification of the wall continues post-mortem (Terashima and Fukushima, 1988; Hosokawa *et al.*, 2001; Pesquet *et al.*, 2013). This requires that the oxidative enzymes are already secreted in the appropriate SCW layer prior to cell death, and that the monolignol supply must come from other sources.

This precisely programmed sequential deposition of hemicelluloses and oxidative enzymes results in a heterogeneous distribution of lignin in SCWs at both the cellular and tissue level. This has been described as the 'topochemistry' of lignin, and it has been revealed by diverse microscopy techniques (reviewed by Donaldson, 2001). Observations of the appearance of lignin in developing wood, using classical histochemistry and fluorescence microscopy, suggested three stages of lignification: deposition in cell corners and compound middle lamella; followed by slow lignification during cellulose and hemicellulose biosynthesis of the thick S2 layer; and finally the bulk of lignin deposition following S3 formation (Donaldson, 2001). The details of lignin composition, including the G-rich nature of the vessels and higher S/G ratio in the fibres, have been mapped with time-of-flight secondary ion mass spectrometry in wood samples from maple (Saito *et al.*, 2012), or with Fourier transform infrared spectroscopy in poplar (Gorzsás *et al.*, 2011). Recently, new lignin imaging technologies, such as fluorescence lifetime imaging, have revealed greater discrimination among fine spatial patterns of lignin heterogeneity in the middle lamella and SCW layers in normal and reaction wood of pine (Donaldson and Radotic, 2013). In addition, the synthesis of fluorescently tagged monolignols that incorporate into lignifying cell walls has permitted direct visualization of monolignol incorporation into lignin polymer (Tobimatsu *et al.*, 2013; Schuetz *et al.*, 2014). The use of click-compatible monolignols is another novel method to identify sites of active lignification in inflorescence stems of arabidopsis, and a combination of click-monolignols with inhibitors was used to demonstrate the requirement for laccases and peroxidases in the lignification of different tissues (Pandey *et al.*, 2016). These techniques relying on incorporation of exogenous monolignols into the cell wall not only confirm the sequence of lignification in cell corners and middle lamella followed by SCW, but they also provide evidence that the mobility of monolignols in the polysaccharide matrix is not limited, as the tagged monolignols appear to diffuse readily through both PCWs and SCWs (Tobimatsu *et al.*, 2013; Schuetz *et al.*, 2014; Pandey *et al.*, 2016). The emerging view of the control underlying the topochemistry of lignin is that lignin composition is dictated by the monolignols made, depending on the transcriptome active in the protoplasts of lignifying cells and neighbours. Monolignols and dimers, and perhaps oligomers, exit the protoplast into the wall where precisely positioned laccases and peroxidases oxidize the subunits into the polymer.

## CONCLUSION

Secondary cell walls are composite materials of cellulose, hemicelluloses and lignin, each deposited in precise and characteristic patterns depending on their physiological function. Thinking about the SCW in a cell biology context helps us to see how these disparate biosynthetic processes are interconnected, relying on many of the same organelles, such as the Golgi and the microtubule-lined SCW domains of the plasma membrane.

There are still many outstanding questions, such as the following. (1) Why are multiple CESA isoforms required to make up a CSC for SCW synthesis? (2) What is the function of the extensive endomembrane population of CESAs, found in Golgi, TGN and SmaCCs/MASCs? (3) Why is the life span of a CSC at the plasma membrane so short and how does this relate to cellulose quality? (4) Are the proteins involved in addition of hemicellulose side chains, and other accessory proteins, incorporated into hemicellulose biosynthetic complexes? (5) How are Golgi-resident biosynthetic proteins recycled during cisternal maturation? (6) Are CSCs, hemicelluloses and laccases/peroxidases packaged into different populations of vesicles at the TGN? (7) How are monolignols exported from the cell? (8) What are the relative roles of laccases and peroxidases in different cell types and tissues?

Perhaps given these myriad questions, it is not surprising that it has been challenging to develop renewable biofuels and bioproducts made from SCW-rich biomass. The bioenergy research world has promoted the study of diverse taxa, such as grasses and poplar, and advanced our understanding of SCW biosynthetic proteins and their products. Learning how these proteins are arranged and controlled by the cell, and how they interact in the Golgi, at the plasma membrane and in the SCW, may provide some unexpected insights that will contribute to exploitation of this carbon-rich renewable resource.

## ACKNOWLEDGEMENTS

The authors thank Vicky Earle for her illustrations. Mendel Perkins, Natalie Hoffman, Jan Xue and Shawn D. Mansfield provided helpful comments on the manuscript. This work was supported by a Discovery Grant to A.L.S., Canada Graduate Scholarship to M.J.M. and Post-Graduate Scholarship to Y.W. from the Canadian Natural Sciences and Engineering Research Council.

## LITERATURE CITED

**Alejandro S**, **Lee Y**, **Tohge T**, ***et al.*** **2012**. AtABCG29 is a monolignol transporter involved in lignin biosynthesis. *Current Biology* **22**: 1207–1212.

**Anderson N**, **Bonawitz ND**, **Nyffeler KE**, **Chapple C. 2015**. Loss of ferulate 5-hydroxylase leads to Mediator-dependent inhibition of soluble phenylpropanoid biosynthesis in Arabidopsis. *Plant Physiology* **169**: 1557–1567.

**Anderson NA**, **Chapple C. 2014**. Perturbing lignin biosynthesis: metabolic changes in response to manipulation of the phenylpropanoid pathway. In: Romani A, Lattanzio V, Quideau S, eds. *Recent advances in polyphenol research*, Vol. **4**. Chichester, UK: John Wiley & Sons, Ltd, 39–59.

**Aoki D**, **Hanaya Y**, **Akita T**, ***et al.*** **2016**. Distribution of coniferin in freeze-fixed stem of *Ginkgo biloba* L. by cryo-TOF-SIMS/SEM. *Scientific Reports* **6**: 31525.

**Arioli T**, **Peng L**, **Betzner AS**, ***et al.*** **1998**. Molecular analysis of cellulose biosynthesis in Arabidopsis. *Science* **279**: 717–720.

**Atmodjo MA**, **Sakuragi Y**, **Zhu X**, ***et al.* 2011**. Galacturonosyltransferase (GAUT)1 and GAUT7 are the core of a plant cell wall pectin biosynthetic homogalacturonan:galacturonosyltransferase complex. *Proceedings of the National Academy of Sciences, USA* **108**: 20225–20230.

**Barros J**, **Serk H**, **Granlund I**, **Pesquet E. 2015**. The cell biology of lignification in higher plants. *Annals of Botany* **115**: 1053–1074.

**Bashline L**, **Li S**, **Anderson CT**, **Lei L**, **Gu Y. 2013**. The endocytosis of cellulose synthase in Arabidopsis is dependent on μ2, a clathrin-mediated endocytosis adaptin. *Plant Physiology* **163**: 150–160.

**Bashline L**, **Li S**, **Gu Y. 2014**. The trafficking of the cellulose synthase complex in higher plants. *Annals of Botany* **114**: 1059–1067.

**Bashline L**, **Li S**, **Zhu X**, **Gu Y. 2015**. The TWD40-2 protein and the AP2 complex cooperate in the clathrin-mediated endocytosis of cellulose synthase to regulate cellulose biosynthesis. *Proceedings of the National Academy of Sciences, USA* **112**: 12870–12875.

**Berthet S**, **Demont-Caulet N**, **Pollet B**, ***et al.* 2011**. Disruption of LACCASE4 and 17 results in tissue-specific alterations to lignification of *Arabidopsis thaliana* stems. *The Plant Cell* **23**: 1124–1137.

**Boija E**, **Johansson G. 2006**. Interactions between model membranes and lignin-related compounds studied by immobilized liposome chromatography. *Biochimica et Biophysica Acta* **1758**: 620–626.

**Boija E**, **Lundquist A**, **Edwards K**, **Johansson G. 2007**. Evaluation of bilayer disks as plant cell membrane models in partition studies. *Analytical Biochemistry* **364**: 145–152.

**Bonawitz ND**, **Chapple C. 2010**. The genetics of lignin biosynthesis: connecting genotype to phenotype. *Annual Review of Genetics* **44**: 337–363.

**Bonawitz ND**, **Soltau WL**, **Blatchley MR**, ***et al.* 2012**. REF4 and RFR1, subunits of the transcriptional coregulatory complex mediator, are required for phenylpropanoid homeostasis in Arabidopsis. *Journal of Biological Chemistry* **287**: 5434–5445.

**Bonawitz ND**, **Kim JI**, **Tobimatsu Y**, ***et al.* 2014**. Disruption of Mediator rescues the stunted growth of a lignin-deficient Arabidopsis mutant. *Nature* **509**: 376–380.

**Bosca S**, **Barton CJ**, **Taylor NG**, ***et al.* 2006**. Interactions between *MUR10/CesA7*-dependent secondary cellulose biosynthesis and primary cell wall structure. *Plant Physiology* **142**: 1353–1363.

**Bowling AJ**, **Brown RM. 2008**. The cytoplasmic domain of cellulose-synthesizing complex in vascular plants. *Protoplasma* **233**: 115–127.

**Bringmann M**, **Li E**, **Sampathkumar A**, **Kocabek T**, **Hauser M-T**, **Persson S. 2012**. POM-POM2/CELLULOSE SYNTHASE INTERACTING1 is essential for the functional association of cellulose synthase and microtubules in Arabidopsis. *The Plant Cell* **24**: 163–177.

**Bromley JR**, **Busse-Wicher M**, **Tryfona T**, ***et al.* 2013**. GUX1 and GUX2 glucuronyltransferases decorate distinct domains of glucuronoxylan with different substitution patterns. *The Plant Journal* **74**: 423–434.

**Brown DM**, **Zeef LAH**, **Ellis J**, **Goodacre R**, **Turner SR. 2005**. Identification of novel genes in Arabidopsis involved in secondary cell wall formation using expression profiling and reverse genetics. *The Plant Cell* **17**: 2281–2295.

**Brown DM**, **Zhang Z**, **Stephens E**, **Dupree P**, **Turner SR. 2009**. Characterization of IRX10 and IRX10-like reveals an essential role in glucuronoxylan biosynthesis in Arabidopsis. *The Plant Journal* **57**: 732–746.

**Campbell MM**, **Sederoff RR. 1996**. Variation in lignin content and composition (mechanisms of control and implications for the genetic improvement of plants). *Plant Physiology* **110**: 3–13.

**Carroll A**, **Specht CD. 2011**. Understanding plant cellulose synthases through a comprehensive investigation of the cellulose synthase family sequences. *Frontiers in Plant Science* **2**: 5.

**Carroll A**, **Mansoori N**, **Li S**, ***et al.* 2012**. Complexes with mixed primary and secondary cellulose synthases are functional in Arabidopsis plants. *Plant Physiology* **160**: 726–737.

**Chen F**, **Duran AL**, **Blount JW**, **Sumner LW**, **Dixon RA. 2003**. Profiling phenolic metabolites in transgenic alfalfa modified in lignin biosynthesis. *Phytochemistry* **64**: 1013–1021.

**Chen F**, **Tobimatsu Y**, **Jackson L**, **Nakashima J**, **Ralph J**, **Dixon RA. 2013**. Novel seed coat lignins in the Cactaceae: structure, distribution and implications for the evolution of lignin diversity. *The Plant Journal* **73**: 201–211.

**Chen S**, **Ehrhardt DW**, **Somerville CR. 2010**. Mutations of cellulose synthase (CESA1) phosphorylation sites modulate anisotropic cell expansion and bidirectional mobility of cellulose synthase. *Proceedings of the National Academy of Sciences, USA* **107**: 17188–17193.

**Chen S**, **Jia H**, **Zhao H**, ***et al.* 2016**. Anisotropic cell expansion is affected through the bidirectional mobility of cellulose synthase complexes and phosphorylation at two critical residues on CESA3. *Plant Physiology* **171**: 242–250.

**Chevalier L**, **Bernard S**, **Ramdani Y**, ***et al.* 2010**. Subcompartment localization of the side chain xyloglucan-synthesizing enzymes within Golgi stacks of tobacco suspension-cultured cells. *The Plant Journal* **64**: 977–989.

**Crowell EF**, **Bischoff V**, **Desprez T**, ***et al.* 2009**. Pausing of Golgi bodies on microtubules regulates secretion of cellulose synthase complexes in Arabidopsis. *The Plant Cell* **21**: 1141–1154.

**Day KJ**, **Staehelin LA**, **Glick BS. 2013**. A three-stage model of Golgi structure and function. *Histochemistry and Cell Biology* **140**: 239–249.

**DeBolt S**, **Gutierrez R**, **Ehrhardt DW**, **Somerville C. 2007**. Nonmotile cellulose synthase subunits repeatedly accumulate within localized regions at the plasma membrane in Arabidopsis hypocotyl cells following 2,6-dichlorobenzonitrile treatment. *Plant Physiology* **145**: 334–338.

**Derbyshire P**, **Ménard D**, **Green P**, ***et al.* 2015**. Proteomic analysis of microtubule interacting proteins over the course of xylem tracheary element formation in Arabidopsis. *The Plant Cell* **27**: 2709–2726.

**Desprez T**, **Juraniec M**, **Crowell EF**, ***et al.* 2007**. Organization of cellulose synthase complexes involved in primary cell wall synthesis in *Arabidopsis thaliana*. *Proceedings of the National Academy of Sciences, USA* **104**: 15572–15577.

**Dima O**, **Morreel K**, **Vanholme B**, **Kim H**, **Ralph J**, **Boerjan W. 2015**. Small glycosylated lignin oligomers are stored in Arabidopsis leaf vacuoles. *The Plant Cell* **27**: 695–710.

**Diotallevi F**, **Mulder B. 2007**. The cellulose synthase complex: a polymerization driven supramolecular motor. *Biophysical Journal* **92**: 2666–2673.

**Dixon RA**, **Srinivasa Reddy MS**, **Gallego-Giraldo L. 2014**. Monolignol biosynthesis and its genetic manipulation: the good, the bad, and the ugly. In: Romani A, Lattanzio V, Quideau S, eds. *Recent advances in polyphenol research*, Vol. **4**. Chichester, UK: John Wiley & Sons, Ltd, 1–38.

**Doblin MS. 2002**. Cellulose biosynthesis in plants: from genes to rosettes. *Plant and Cell Physiology* **43**: 1407–1420.

**Donaldson LA. 2001**. Lignification and lignin topochemistry – an ultrastructural view. *Phytochemistry* **57**: 859–873.

**Donaldson LA**, **Knox JP. 2012**. Localization of cell wall polysaccharides in normal and compression wood of radiata pine: relationships with lignification and microfibril orientation. *Plant Physiology* **158**: 642–653.

**Donaldson LA**, **Radotic K. 2013**. Fluorescence lifetime imaging of lignin autofluorescence in normal and compression wood. *Journal of Microscopy* **251**: 178–187.

**Ebert B**, **Rautengarten C**, **Guo X**, ***et al.* 2015**. Identification and characterization of a Golgi-localized UDP-xylose transporter family from Arabidopsis. *The Plant Cell* **27**: 1218–1227.

**Ebringerová A. 2005**. Structural diversity and application potential of hemicelluloses. *Macromolecular Symposia* **232**: 1–12.

**Ehlting J**, **Mattheus N**, **Aeschliman DS**, ***et al.* 2005**. Global transcript profiling of primary stems from *Arabidopsis thaliana* identifies candidate genes for missing links in lignin biosynthesis and transcriptional regulators of fiber differentiation. *The Plant Journal* **42**: 618–640.

**Endler A**, **Kesten C**, **Schneider R**, ***et al.* 2015**. A mechanism for sustained cellulose synthesis during salt stress. *Cell* **162**: 1353–1364.

**Endo S**, **Pesquet E**, **Yamaguchi M**, ***et al.* 2009**. Identifying new components participating in the secondary cell wall formation of vessel elements in Zinnia and Arabidopsis. *The Plant Cell* **21**: 1155–1165.

**Engel BD**, **Schaffer M**, **Albert S**, **Asano S**, **Plitzko JM**, **Baumeister W. 2015**. *In situ* structural analysis of Golgi intracisternal protein arrays. *Proceedings of the National Academy of Sciences, USA* **112**: 11264–11269.

**Fernandes AN**, **Thomas LH**, **Altaner CM**, ***et al.* 2011**. Nanostructure of cellulose microfibrils in spruce wood. *Proceedings of the National Academy of Sciences, USA* **108**: E1195–E1203.

**Fernández-Pérez F**, **Pomar F**, **Pedreño MA**, **Novo-Uzal E. 2015*a***. The suppression of AtPrx52 affects fibers but not xylem lignification in Arabidopsis by altering the proportion of syringyl units. *Physiologia Plantarum* **154**: 395–406.

**Fernández-Pérez F**, **Pomar F**, **Pedreño MA**, **Novo-Uzal E. 2015*b***. Suppression of Arabidopsis peroxidase 72 alters cell wall and phenylpropanoid metabolism. *Plant Science* **239**: 192–199.

**Fisher DD**, **Cyr RJ. 1998**. Extending the microtubule/microfibril paradigm. *Plant Physiology* **116**: 1043–1051.

**Freudenberg K. 1965**. Lignin: its constitution and formation from p-hydroxycinnamyl alcohols. *Science* **148**: 595–600.

**Fujimoto M**, **Suda Y**, **Vernhettes S**, **Nakano A**, **Ueda T. 2015**. Phosphatidylinositol 3-kinase and 4-kinase have distinct roles in intracellular trafficking of cellulose synthase complexes in *Arabidopsis thaliana*. *Plant and Cell Physiology* **56**: 287–298.

**Fujita M**, **Himmelspach R**, **Hocart CH**, **Williamson RE**, **Mansfield SD**, **Wasteneys GO. 2011**. Cortical microtubules optimize cell-wall crystallinity to drive unidirectional growth in Arabidopsis. *The Plant Journal* **66**: 915–928.

**Gardiner JC**, **Taylor NG**, **Turner SR. 2003**. Control of cellulose synthase complex localization in developing xylem. *The Plant Cell* **15**: 1740–1748.

**Gendre D**, **McFarlane HE**, **Johnson E**, ***et al.* 2013**. Trans-Golgi network localized ECHIDNA/Ypt interacting protein complex is required for the secretion of cell wall polysaccharides in Arabidopsis. *The Plant Cell* **25**: 2633–2646.

**Gendre D**, **Jonsson K**, **Boutté Y**, **Bhalerao RP. 2015**. Journey to the cell surface – the central role of the trans-Golgi network in plants. *Protoplasma* **252**: 385–398.

**Giddings TH**, **Brower DL**, **Staehelin LA. 1980**. Visualization of particle complexes in the plasma membrane of *Micrasterias denticulata* associated with the formation of cellulose fibrils in primary and secondary cell walls. *Journal of Cell Biology* **84**: 327–339.

**Glick BS**, **Luini A. 2011**. Models for Golgi traffic: a critical assessment. *Cold Spring Harbor Perspectives in Biology* **3**: 1–15.

**Gonneau M**, **Desprez T**, **Guillot A**, **Vernhettes S**, **Hofte H. 2014**. Catalytic subunit stoichiometry within the cellulose synthase complex. *Plant Physiology* **166**: 1709–1712.

**Gorshkova T**, **Brutch N**, **Chabbert B**, **Deyholos M**, **Hayashi T**, **Lev-Yadun S. 2012**. Plant fiber formation: state of the art, recent expected progress, and open questions. *Critical Reviews in Plant Sciences* **31**: 201–228.

**Gorzsás A**, **Stenlund H**, **Persson P**, **Trygg J**, **Sundberg B. 2011**. Cell-specific chemotyping and multivariate imaging by combined FT-IR microspectroscopy and orthogonal projections to latent structures (OPLS) analysis reveals the chemical landscape of secondary xylem. *The Plant Journal* **66**: 903–914.

**Gu Y**, **Kaplinsky N**, **Bringmann M**, ***et al.* 2010**. Identification of a cellulose synthase-associated protein required for cellulose biosynthesis. *Proceedings of the National Academy of Sciences, USA* **107**: 12866–12871.

**Guerriero G**, **Fugelstad J**, **Bulone V. 2010**. What do we really know about cellulose biosynthesis in higher plants? *Journal of Integrative Plant Biology* **52**: 161–175.

**Gutierrez R**, **Lindeboom JJ**, **Paredez AR**, **Emons AMC**, **Ehrhardt DW. 2009**. Arabidopsis cortical microtubules position cellulose synthase delivery to the plasma membrane and interact with cellulose synthase trafficking compartments. *Nature Cell Biology* **11**: 797–806.

**Haigler CH**, **Brown RM. 1986**. Transport of rosettes from the Golgi apparatus to the plasma membrane in isolated mesophyll cells of *Zinnia elegans*. *Protoplasma* **134**: 111–120.

**Hao Z**, **Mohnen D. 2014**. A review of xylan and lignin biosynthesis: foundation for studying Arabidopsis irregular xylem mutants with pleiotropic phenotypes. *Critical Reviews in Biochemistry and Molecular Biology* **49**: 212–241.

**Haughn GW**, **Western TL. 2012**. Arabidopsis seed coat mucilage is a specialized cell wall that can be used as a model for genetic analysis of plant cell wall structure and function. *Frontiers in Plant Science* **3**: 1–5.

**Heilmann M**, **Heilmann I. 2015**. Plant phosphoinositides – complex networks controlling growth and adaptation. *Biochimica et Biophysica Acta* **1851**: 759–769.

**Hepler PK**, **Fosket DE. 1971**. The role of microtubules in vessel member differentiation in Coleus. *Protoplasma* **72**: 213–236.

**Herrero J**, **Fernández-Pérez F**, **Yebra T**, ***et al.* 2013**. Bioinformatic and functional characterization of the basic peroxidase 72 from *Arabidopsis thaliana* involved in lignin biosynthesis. *Planta* **237**: 1599–1612.

**Herth W. 1980**. Calcofluor white and Congo red inhibit chitin microfibril assembly of *Poterioochromonas*: evidence for a gap between polymerization and microfibril formation. *Journal of Cell Biology* **87**: 442–450.

**Herth W. 1985**. Plasma-membrane rosettes involved in localized wall thickening during xylem vessel formation of *Lepidium sativum* L. *Planta* **164**: 12–21.

**Hill JL**, **Hammudi MB**, **Tien M. 2014**. The Arabidopsis cellulose synthase complex: a proposed hexamer of CESA trimers in an equimolar stoichiometry. *The Plant Cell* **26**: 4834–4842.

**Hon DNS. 1994**. Cellulose: a random walk along its historical path. *Cellulose* **1**: 1–25.

**Hosokawa M**, **Suzuki S**, **Umezawa T**, **Sato Y. 2001**. Progress of lignification mediated by intercellular transportation of monolignols during tracheary element differentiation of isolated *Zinnia* mesophyll cells. *Plant and Cell Physiology* **42**: 959–968.

**Huis R**, **Morreel K**, **Fliniaux O**, ***et al.* 2012**. Natural hypolignification is associated with extensive oligolignol accumulation in flax stems. *Plant Physiology* **158**: 1893–1915.

**Ito Y**, **Uemura T**, **Nakano A. 2014**. Formation and maintenance of the Golgi apparatus in plant cells. *International Review of Cell and Molecular Biology* **310**: 221–287.

**Jacob-Wilk D**, **Kurek I**, **Hogan P**, **Delmer DP. 2006**. The cotton fiber zinc-binding domain of cellulose synthase A1 from *Gossypium hirsutum* displays rapid turnover *in vitro* and *in vivo*. *Proceedings of the National Academy of Sciences, USA* **103**: 12191–12196.

**Jaini R**, **Wang P**, **Dudareva N**, **Chapple C**, **Morgan JA. 2017**. Targeted metabolomics of the phenylpropanoid pathway in *Arabidopsis thaliana* using reversed phase liquid chromatography coupled with tandem mass spectrometry. *Phytochemical Analysis* **28**: 267–276.

**Jensen JK**, **Johnson NR**, **Wilkerson CG. 2014**. *Arabidopsis thaliana* IRX10 and two related proteins from psyllium and *Physcomitrella patens* are xylan xylosyltransferases. *The Plant Journal* **80**: 207–215.

**Kaneda M**, **Rensing KH**, **Wong JCT**, **Banno B**, **Mansfield SD**, **Samuels AL. 2008**. Tracking monolignols during wood development in lodgepole pine. *Plant Physiology* **147**: 1750–1760.

**Kaneda M**, **Schuetz M**, **Lin B.**, ***et al.* 2011**. ABC transporters coordinately expressed during lignification of Arabidopsis stems include a set of ABCBs associated with auxin transport. *Journal of Experimental Botany* **62**: 2063–2077.

**Kang B-H**, **Nielsen E**, **Preuss ML**, **Mastronarde D**, **Staehelin LA. 2011**. Electron tomography of RabA4b- and PI-4Kβ1-labeled trans Golgi network compartments in Arabidopsis. *Traffic* **12**: 313–329.

**Keppler BD**, **Showalter AM. 2010**. IRX14 and IRX14-LIKE, two glycosyl transferases involved in glucuronoxylan biosynthesis and drought tolerance in Arabidopsis. *Molecular Plant* **3**: 834–841.

**Kim JS**, **Awano T**, **Yoshinaga A**, **Takabe K. 2010**. Immunolocalization of β-1–4-galactan and its relationship with lignin distribution in developing compression wood of *Cryptomeria japonica*. *Planta* **232**: 109–119.

**Kim JS**, **Awano T**, **Yoshinaga A**, **Takabe K. 2011**. Occurrence of xylan and mannan polysaccharides and their spatial relationship with other cell wall components in differentiating compression wood tracheids of *Cryptomeria japonica*. *Planta* **233**: 721–735.

**Kim SH**, **Lee CM**, **Kafle K. 2013**. Characterization of crystalline cellulose in biomass: basic principles, applications, and limitations of XRD, NMR, IR, Raman, and SFG. *Korean Journal of Chemical Engineering* **30**: 2127–2141.

**Kim SJ**, **Brandizzi F. 2016**. The plant secretory pathway for the trafficking of cell wall polysaccharides and glycoproteins. *Glycobiology* **26**: 940–949.

**Kimura S**, **Laosinchai W**, **Itoh T**, **Cui X**, **Linder C**, **Brown R. 1999**. Immunogold labeling of rosette terminal cellulose-synthesizing complexes in the vascular plant *Vigna angularis*. *The Plant Cell* **11**: 2075–2086.

**Klute MJ**, **Melançon P**, **Dacks JB. 2011**. Evolution and diversity of the Golgi. *Cold Spring Harbor Perspectives in Biology* **3**: a007849.

**Kobayashi H**, **Fukuda H**, **Shibaoka H. 1988**. Interrelation between the spatial disposition of actin filaments and microtubules during the differentiation of tracheary elements in cultured Zinnia cells. *Protoplasma* **143**: 29–37.

**Krishnamoorthy P**, **Sanchez-Rodriguez C**, **Heilmann I**, **Persson S. 2014**. Regulatory roles of phosphoinositides in membrane trafficking and their potential impact on cell-wall synthesis and re-modelling. *Annals of Botany* **114**: 1049–1057.

**Kuang B**, **Zhao X**, **Zhou C**, ***et al.* 2016**. The role of UDP-glucuronic acid decarboxylase (UXS) in xylan biosynthesis in Arabidopsis. *Molecular Plant* **9**: 1119–1131.

**Kumar M**, **Campbell L**, **Turner S. 2016*a***. Secondary cell walls: biosynthesis and manipulation. *Journal of Experimental Botany* **67**: 515–531.

**Kumar M**, **Wightman R**, **Atanassov I**, ***et al.* 2016*b***. S-Acylation of the cellulose synthase complex is essential for its plasma membrane localization. *Science* **353**: 166–169.

**Kumar M**, **Atanassov I**, **Turner S. 2017**. Functional analysis of cellulose synthase (CESA) protein class specificity. *Plant Physiology* **173**: 970–983.

**Laitinen T**, **Morreel K**, **Delhomme N**, ***et al.* 2017**. A key role for apoplastic $H_2O_2$ in Norway spruce phenolic metabolism. *Plant Physiology* **174**: 1449–1475.

**Lane DR**, **Wiedemeier A**, **Peng L**, ***et al.* 2001**. Temperature-sensitive alleles of RSW2 link the KORRIGAN endo-1,4-β-glucanase to cellulose synthesis and cytokinesis in Arabidopsis. *Plant Physiology* **126**: 278–288.

**Le Roy J**, **Huss B**, **Creach A**, **Hawkins S**, **Neutelings G. 2016**. Glycosylation is a major regulator of phenylpropanoid availability and biological activity in plants. *Frontiers in Plant Science* **7**: 735.

**Ledbetter MCC**, **Porter KRR. 1963**. A 'microtubule' in plant cell fine structure. *Journal of Cell Biology* **19**: 239–250.

**Lee C**, **Teng Q**, **Huang W**, **Zhong R**, **Ye Z-H. 2010**. The Arabidopsis family GT43 glycosyltransferases form two functionally nonredundant groups essential for the elongation of glucuronoxylan backbone. *Plant Physiology* **153**: 526–541.

**Lee Y**, **Rubio MC**, **Alassimone J**, **Geldner N. 2013**. A mechanism for localized lignin deposition in the endodermis. *Cell* **153**: 402–412.

**Lei L**, **Li S**, **Gu Y. 2012**. Cellulose synthase interactive protein 1 (CSI1) mediates the intimate relationship between cellulose microfibrils and cortical microtubules. *Plant Signaling and Behavior* **7**: 714–718.

**Lei L**, **Li S**, **Du J**, **Bashline L**, **Gu Y. 2013**. CELLULOSE SYNTHASE INTERACTIVE3 regulates cellulose biosynthesis in both a microtubule-dependent and microtubule-independent manner in Arabidopsis. *The Plant Cell* **25**: 4912–4923.

**Lei L**, **Zhang T**, **Strasser R**, ***et al.* 2014**. The jiaoyao1 mutant is an allele of korrigan1 that abolishes endoglucanase activity and affects the organization of both cellulose microfibrils and microtubules in Arabidopsis. *The Plant Cell* **26**: 2601–2616.

**Li S**, **Lei L**, **Somerville CR**, **Gu Y. 2012**. Cellulose synthase interactive protein 1 (CSI1) links microtubules and cellulose synthase complexes. *Proceedings of the National Academy of Sciences, USA* **109**: 185–190.

**Li S**, **Chen M**, **Yu D**, ***et al.* 2013**. EXO70A1-mediated vesicle trafficking is critical for tracheary element development in Arabidopsis. *The Plant Cell* **25**: 1774–1786.

**Li S**, **Bashline L**, **Zheng Y**, ***et al.* 2016**. Cellulose synthase complexes act in a concerted fashion to synthesize highly aggregated cellulose in secondary cell walls of plants. *Proceedings of the National Academy of Sciences, USA* **113**: 11348–11353.

**Li X**, **Chapple C. 2010**. Understanding lignification: challenges beyond monolignol biosynthesis. *Plant Physiology* **154**: 449–452.

**Li Y**, **Qian Q**, **Zhou Y**, ***et al.* 2003**. BRITTLE CULM1, which encodes a COBRA-like protein, affects the mechanical properties of rice plants. *The Plant Cell* **15**: 2020–2031.

**Li Z**, **Fernie AR**, **Persson S. 2016**. Transition of primary to secondary cell wall synthesis. *Science Bulletin* **61**: 838–846.

**Liu L**, **Shang-Guan K**, **Zhang B**, ***et al.* 2013**. Brittle culm1, a COBRA-like protein, functions in cellulose assembly through binding cellulose microfibrils. *PLoS Genetics* **9**: e1003704.

**Liu Z**, **Schneider R**, **Kesten C**, ***et al.* 2016**. Cellulose–microtubule uncoupling proteins prevent lateral displacement of microtubules during cellulose synthesis in Arabidopsis. *Developmental Cell* **38**: 305–315.

**Lund CH**, **Bromley JR**, **Stenbæk A**, **Rasmussen RE**, **Scheller HV**, **Sakuragi Y. 2015**. A reversible Renilla luciferase protein complementation assay for rapid identification of protein–protein interactions reveals the existence of an interaction network involved in xyloglucan biosynthesis in the plant Golgi apparatus. *Journal of Experimental Botany* **66**: 85–97.

**MacAdam JW**, **Nelson CJ. 2002**. Secondary cell wall deposition causes radial growth of fibre cells in the maturation zone of elongating tall fescue leaf blades. *Annals of Botany* **89**: 89–96.

**Maloney VJ**, **Mansfield SD. 2010**. Characterization and varied expression of a membrane-bound endo-β-1,4-glucanase in hybrid poplar. *Plant Biotechnology Journal* **8**: 294–307.

**Maloney VJ**, **Samuels AL**, **Mansfield SD. 2012**. The endo-1,4-β-glucanase Korrigan exhibits functional conservation between gymnosperms and angiosperms and is required for proper cell wall formation in gymnosperms. *New Phytologist* **193**: 1076–1087.

**Mansoori N**, **Timmers J**, **Desprez T**, ***et al.* 2014**. KORRIGAN1 interacts specifically with integral components of the cellulose synthase machinery. *PLoS One* **9**: e112387.

**Marriott PE**, **Gómez LD**, **McQueen-Mason SJ. 2016**. Unlocking the potential of lignocellulosic biomass through plant science. *New Phytologist* **209**: 1366–1381.

**McFarlane HE**, **Watanabe Y**, **Gendre D**, ***et al.* 2013**. Cell wall polysaccharides are mislocalized to the vacuole in echidna mutants. *Plant and Cell Physiology* **54**: 1867–1880.

**McFarlane HE**, **Döring A**, **Persson S. 2014**. The cell biology of cellulose synthesis. *Annual Review of Plant Biology* **65**: 69–94.

**McNeil M**, **Darvill AG**, **Fry SC**, **Albersheim P. 1984**. Structure and function of the primary cell walls of plants. *Annual Review of Biochemistry* **53**: 625–663.

**Miao Y-C**, **Liu C-J. 2010**. ATP-binding cassette-like transporters are involved in the transport of lignin precursors across plasma and vacuolar membranes. *Proceedings of the National Academy of Sciences, USA* **107**: 22728–22733.

**Miart F**, **Desprez T**, **Biot E**, ***et al.* 2014**. Spatio-temporal analysis of cellulose synthesis during cell plate formation in Arabidopsis. *The Plant Journal* **77**: 71–84.

**Morgan JLW**, **Strumillo J**, **Zimmer J. 2013**. Crystallographic snapshot of cellulose synthesis and membrane translocation. *Nature* **493**: 181–186.

**Morreel K**, **Ralph J**, **Kim H**, ***et al.* 2004**. Profiling of oligolignols reveals monolignol coupling conditions in lignifying poplar xylem. *Plant Physiology* **136**: 3537–3549.

**Mottiar Y**, **Vanholme R**, **Boerjan W**, **Ralph J**, **Mansfield SD. 2016**. Designer lignins: harnessing the plasticity of lignification. *Current Opinion in Biotechnology* **37**: 190–200.

**Mueller SC**, **Brown RM. 1980**. Evidence for an intramembrane component associated with a cellulose microfibril-synthesizing complex in higher plants. *Journal of Cell Biology* **84**: 315–326.

**Nakano Y**, **Yamaguchi M**, **Endo H**, **Rejab NA**, **Ohtani M. 2015**. NAC-MYB-based transcriptional regulation of secondary cell wall biosynthesis in land plants. *Frontiers in Plant Science* **6**: 288.

**Newman RH**, **Hill SJ**, **Harris PJ. 2013**. Wide-angle X-ray scattering and solid-state nuclear magnetic resonance data combined to test models for cellulose microfibrils in mung bean cell walls. *Plant Physiology* **163**: 1558–1567.

**Niculaes C**, **Morreel K**, **Kim H**, ***et al.* 2014**. Phenylcoumaran benzylic ether reductase prevents accumulation of compounds formed under oxidative conditions in poplar xylem. *The Plant Cell* **26**: 3775–3791.

**Nixon BT**, **Mansouri K**, **Singh A**, ***et al.* 2016**. Comparative structural and computational analysis supports eighteen cellulose synthases in the plant cellulose synthesis complex. *Scientific Reports* **6**: 28696.

**Oda Y**, **Fukuda H. 2012**. Initiation of cell wall pattern by a Rho- and microtubule-driven symmetry breaking. *Science* **337**: 1333–1336.

**Oda Y**, **Fukuda H. 2013**. Rho of plant GTPase signaling regulates the behavior of Arabidopsis Kinesin-13A to establish secondary cell wall patterns. *The Plant Cell* **25**: 4439–4450.

**Oda Y**, **Iida Y**, **Nagashima Y**, **Sugiyama Y**, **Fukuda H. 2015**. Novel coiled-coil proteins regulate exocyst association with cortical microtubules in xylem cells via the conserved oligomeric Golgi-complex 2 protein. *Plant and Cell Physiology* **56**: 277–286.

**Oehme DP**, **Downton MT**, **Doblin MS**, **Wagner J**, **Gidley MJ**, **Bacic A. 2015**. Unique aspects of the structure and dynamics of elementary Iβ cellulose microfibrils revealed by computational simulations. *Plant Physiology* **168**: 3–17.

**Oikawa A**, **Lund CH**, **Sakuragi Y**, **Scheller HV. 2013**. Golgi-localized enzyme complexes for plant cell wall biosynthesis. *Trends in Plant Science* **1**: 49–58.

**Omadjela O**, **Narahari A**, **Strumillo J**, ***et al.* 2013**. BcsA and BcsB form the catalytically active core of bacterial cellulose synthase sufficient for *in vitro* cellulose synthesis. *Proceedings of the National Academy of Sciences, USA* **110**: 17856–17861.

**Pandey JL**, **Kiemle SN**, **Richard TL**, **Zhu Y**, **Cosgrove DJ**, **Anderson CT. 2016**. Investigating biochemical and developmental dependencies of lignification with a click-compatible monolignol analog in *Arabidopsis thaliana* stems. *Frontiers in Plant Science* **7**: 1–15.

**Paredez AR**, **Somerville C**, **Ehrhardt D. 2006**. Visualization of cellulose synthase with microtubules. *Science* **312**: 1491–1495.

**Paredez AR**, **Persson S**, **Ehrhardt DW**, **Somerville CR. 2008**. Genetic evidence that cellulose synthase activity influences microtubule cortical array organization. *Plant Physiology* **147**: 1723–1734.

**Park S-Y**, **Yang J-S**, **Schmider AB**, **Soberman RJ**, **Hsu VW. 2015**. Coordinated regulation of bidirectional COPI transport at the Golgi by CDC42. *Nature* **521**: 529–532.

**Pawar PM-A**, **Koutaniemi S**, **Tenkanen M**, **Mellerowicz EJ. 2013**. Acetylation of woody lignocellulose: significance and regulation. *Frontiers in Plant Science* **4**: 118.

**Pear JR**, **Kawagoe Y**, **Schreckengost WE**, **Delmer DP**, **Stalker DM. 1996**. Higher plants contain homologs of the bacterial celA genes encoding the catalytic subunit of cellulose synthase. *Proceedings of the National Academy of Sciences, USA* **93**: 12637–12642.

**Peña MJ**, **Kulkarni AR**, **Backe J**, **Boyd M**, **O'Neill MA**, **York WS. 2016**. Structural diversity of xylans in the cell walls of monocots. *Planta* **244**: 589–606.

**Peña MJ**, **Zhong R**, **Zhou G-K**, ***et al.* 2007**. Arabidopsis irregular xylem8 and irregular xylem9: implications for the complexity of glucuronoxylan biosynthesis. *The Plant Cell* **19**: 549–563.

**Persson S**, **Wei H**, **Milne J**, **Page GP**, **Somerville CR. 2005**. Identification of genes required for cellulose synthesis by regression analysis of public microarray data sets. *Proceedings of the National Academy of Sciences, USA* **102**: 8633–8638.

**Pesquet E**, **Zhang B**, **Gorzsas A**, ***et al.* 2013**. Non-cell-autonomous postmortem lignification of tracheary elements in *Zinnia elegans*. *The Plant Cell* **25**: 1314–1328.

**Pickett-Heaps JD. 1968**. Xylem wall deposition. *Protoplasma* **65**: 181–201.

**Purushotham P**, **Cho SH**, **Díaz-Moreno SM**, ***et al.* 2016**. A single heterologously expressed plant cellulose synthase isoform is sufficient for cellulose microfibril formation *in vitro*. *Proceedings of the National Academy of Sciences, USA* **113**: 11360–11365.

**Ragauskas AJ**, **Beckham GT**, **Biddy MJ**, ***et al.* 2014**. Lignin valorization: improving lignin processing in the biorefinery. *Science* **344**: 1246843–1246843.

**Rejab NA**, **Nakano Y**, **Yoneda A**, **Ohtani M**, **Demura T. 2015**. Possible contribution of TED6 and TED7, secondary cell wall-related membrane proteins, to evolution of tracheary element in angiosperm lineage. *Plant Biotechnology* **32**: 343–347.

**Ren Y**, **Hansen SF**, **Ebert B**, **Lau J**, **Scheller HV. 2014**. Site-directed mutagenesis of IRX9, IRX9L and IRX14 proteins involved in xylan biosynthesis: glycosyltransferase activity is not required for IRX9 function in Arabidopsis. *PLoS One* **9**: e105014.

**Rennie EA**, **Scheller HV. 2014**. Xylan biosynthesis. *Current Opinion in Biotechnology* **26**: 100–107.

**Rizzo R**, **Parashuraman S**, **Mirabelli P**, **Puri C**, **Lucocq J**, **Luini A. 2013**. The dynamics of engineered resident proteins in the mammalian Golgi complex relies on cisternal maturation. *Journal of Cell Biology* **201**: 1027–1036.

**Rodríguez-Gacio MDC**, **Iglesias-Fernández R**, **Carbonero P**, **Matilla AJ. 2012**. Softening-up mannan-rich cell walls. *Journal of Experimental Botany* **63**: 3976–3988.

**Rudolph U. 1987**. Occurrence of rosettes in the ER membrane of young *Funaria hygrometrica* protonemata. *Naturwissenschaften* **74**: 439–439.

**Rudolph U**, **Schnepf E. 1988**. Investigations of the turnover of the putative cellulose-synthesizing particle 'rosettes' within the plasma membrane of *Funaria hygrometrica* protonema cells – I. Effects of monensin and cytochalasin B. *Protoplasma* **143**: 63–73.

**Saito K**, **Watanabe Y**, **Shirakawa M**, ***et al.* 2012**. Direct mapping of morphological distribution of syringyl and guaiacyl lignin in the xylem of maple by time-of-flight secondary ion mass spectrometry. *The Plant Journal* **69**: 542–552.

**Sampathkumar A**, **Gutierrez R**, **McFarlane HE**, ***et al.* 2013**. Patterning and lifetime of plasma membrane-localized cellulose synthase is dependent on actin organization in Arabidopsis interphase cells. *Plant Physiology* **162**: 675–688.

**Samuels AL**, **Rensing KH**, **Douglas CJ**, **Mansfield SD**, **Dharmawardhana DP**, **Ellis BE. 2002**. Cellular machinery of wood production: differentiation of secondary xylem in *Pinus contorta* var. *latifolia*. *Planta* **216**: 72–82.

**Sánchez-Rodríguez C**, **Bauer S**, **Hematy K**, ***et al.* 2012**. CHITINASE-LIKE1/POM-POM1 and its homolog CTL2 are glucan-interacting proteins important for cellulose biosynthesis in Arabidopsis. *The Plant Cell* **24**: 589–607.

**Sánchez-Rodríguez C**, **Ketelaar K**, **Schneider R**, ***et al.* 2017**. BRASSINOSTEROID INSENSITIVE2 negatively regulates cellulose synthesis in Arabidopsis by phosphorylating cellulose synthase 1. *Proceedings of the National Academy of Sciences, USA* **114**: 3533–3538.

**Sato SS**, **Kato T**, **Kakegawa K**, ***et al.* 2001**. Role of the putative membrane-bound endo-1,4-beta-glucanase KORRIGAN in cell elongation and cellulose synthesis in *Arabidopsis thaliana*. *Plant and Cell Physiology* **42**: 251–263.

**Savidge RA. 1989**. Coniferin, a biochemical indicator of commitment to tracheid differentiation in conifers. *Canadian Journal of Botany* **67**: 2663–2668.

**Scheller HV**, **Ulvskov P. 2010**. Hemicelluloses. *Annual Review of Plant Biology* **61**: 263–289.

**Schneider R**, **Tang L**, **Lampugnani ER**, ***et al.* 2017**. Two complementary mechanisms underpin cell wall patterning during xylem vessel development. *The Plant Cell* **29**: 2433–2449.

**Schoberer J**, **Strasser R. 2011**. Sub-compartmental organization of Golgi-resident N-glycan processing enzymes in plants. *Molecular Plant* **4**: 220–228.

**Schuetz M**, **Benske A**, **Smith RA**, ***et al.* 2014**. Laccases direct lignification in the discrete secondary cell wall domains of protoxylem. *Plant Physiology* **166**: 798–807.

**Sethaphong L**, **Davis JK**, **Slabaugh E**, **Singh A**, **Haigler CH**, **Yingling YG. 2015**. Prediction of the structures of the plant-specific regions of vascular plant cellulose synthases and correlated functional analysis. *Cellulose* **23**: 145–161.

**Shigeto J**, **Tsutsumi Y. 2016**. Diverse functions and reactions of class III peroxidases. *New Phytologist* **209**: 1395–1402.

**Shigeto J**, **Itoh Y**, **Hirao S**, **Ohira K**, **Fujita K**, **Tsutsumi Y. 2015**. Simultaneously disrupting AtPrx2, AtPrx25 and AtPrx71 alters lignin content and structure in Arabidopsis stem. *Journal of Integrative Plant Biology* **57**: 349–356.

**Simmons TJ**, **Mortimer JC**, **Bernardinelli OD**, ***et al.* 2016**. Folding of xylan onto cellulose fibrils in plant cell walls revealed by solid-state NMR. *Nature Communications* **7**: 13902.

**Slabaugh E**, **Davis JK**, **Haigler CH**, **Yingling YG**, **Zimmer J. 2014**. Cellulose synthases: new insights from crystallography and modeling. *Trends in Plant Science* **19**: 99–106.

**Smith RA**, **Schuetz M**, **Roach M**, **Mansfield SD**, **Ellis B**, **Samuels L. 2013**. Neighboring parenchyma cells contribute to Arabidopsis xylem lignification, while lignification of interfascicular fibers is cell autonomous. *The Plant Cell* **25**: 3988–3999.

**Smith RA**, **Schuetz M**, **Karlen SD**, ***et al.* 2017**. Defining the diverse cell populations contributing to lignification in *Arabidopsis thaliana* stems. *Plant Physiology* **174**: 1028–1036.

**Staehelin LA**, **Giddings TH**, **Kiss JZ**, **Sack FD. 1990**. Macromolecular differentiation of Golgi stacks in root tips of Arabidopsis and Nicotiana seedlings as visualized in high pressure frozen and freeze-substituted samples. *Protoplasma* **157**: 75–91.

**Synek L**, **Sekereš J**, **Žárský V. 2014**. The exocyst at the interface between cytoskeleton and membranes in eukaryotic cells. *Frontiers in Plant Science* **4**: 543.

**Szyjanowicz PMJ**, **McKinnon I**, **Taylor NG**, **Gardiner J**, **Jarvis MC**, **Turner SR. 2004**. The irregular xylem 2 mutant is an allele of korrigan that affects the secondary cell wall of *Arabidopsis thaliana*. *The Plant Journal* **37**: 730–740.

**Taylor NG. 2007**. Identification of cellulose synthase AtCesA7 (IRX3) in vivo phosphorylation sites – a potential role in regulating protein degradation. *Plant Molecular Biology* **64**: 161–171.

**Taylor NG**, **Scheible W-R**, **Cutler S**, **Somerville CR**, **Turner SR. 1999**. The irregular xylem3 locus of Arabidopsis encodes a cellulose synthase required for secondary cell wall synthesis. *The Plant Cell* **11**: 769–779.

**Taylor NG**, **Laurie S**, **Turner SR. 2000**. Multiple cellulose synthase catalytic subunits are required for cellulose synthesis in Arabidopsis. *The Plant Cell* **12**: 2529–2539.

**Taylor NG**, **Howells RM**, **Huttly AK**, **Vickers K**, **Turner SR. 2003**. Interactions among three distinct CesA proteins essential for cellulose synthesis. *Proceedings of the National Academy of Sciences, USA* **100**: 1450–1455.

**Taylor-Teeples M**, **Lin L**, **de Lucas M**, ***et al.* 2014**. An Arabidopsis gene regulatory network for secondary cell wall synthesis. *Nature* **517**: 571–575.

**Terashima N**, **Fukushima K. 1988**. Heterogeneity in formation of lignin-XI: an autoradiographic study of the heterogeneous formation and structure of pine lignin. *Wood Science and Technology* **22**: 259–270.

**Terashima N**, **Ko C**, **Matsushita Y**, **Westermark U. 2016**. Monolignol glucosides as intermediate compounds in lignin biosynthesis. Revisiting the cell wall lignification and new 13C-tracer experiments with *Ginkgo biloba* and *Magnolia liliiflora*. *Holzforschung* **70**: 801–810.

**Thomas LH**, **Forsyth VT**, **Sturcova A**, ***et al.* 2013**. Structure of cellulose microfibrils in primary cell walls from collenchyma. *Plant Physiology* **161**: 465–476.

**Tobimatsu Y**, **Wagner A**, **Donaldson L**, ***et al.* 2013**. Visualization of plant cell wall lignification using fluorescence-tagged monolignols. *The Plant Journal* **76**: 357–366.

**Tominaga M**, **Ito K. 2015**. The molecular mechanism and physiological role of cytoplasmic streaming. *Current Opinion in Plant Biology* **27**: 104–110.

**Toyooka K**, **Sato M**, **Kutsuna N**, ***et al.* 2014**. Wide-range high-resolution transmission electron microscopy reveals morphological and distributional changes of endomembrane compartments during log to stationary transition of growth phase in tobacco BY-2 cells. *Plant and Cell Physiology* **55**: 1544–1555.

**Tsuji Y**, **Chen F**, **Yasuda S**, **Fukushima K. 2004**. The behavior of deuterium-labeled monolignol and monolignol glucosides in lignin biosynthesis in angiosperms. *Journal of Agricultural and Food Chemistry* **52**: 131–134.

**Tsuyama T**, **Takabe K. 2014**. Distribution of lignin and lignin precursors in differentiating xylem of Japanese cypress and poplar. *Journal of Wood Science* **60**: 353–361.

**Tsuyama T**, **Kawai R**, **Shitan N**, ***et al.* 2013**. Proton-dependent coniferin transport, a common major transport event in differentiating xylem tissue of woody plants. *Plant Physiology* **162**: 918–926.

**Turner SR**, **Somerville CR. 1997**. Collapsed xylem phenotype of Arabidopsis identifies mutants deficient in cellulose deposition in the secondary cell wall. *The Plant Cell* **9**: 689–701.

**Uemura T. 2016**. Physiological roles of plant post-Golgi transport pathways in membrane trafficking. *Plant and Cell Physiology* **57**: 2013–2019.

**Urbanowicz BR**, **Peña MJ**, **Moniz HA**, **Moremen KW**, **York WS. 2014**. Two Arabidopsis proteins synthesize acetylated xylan *in vitro*. *The Plant Journal* **80**: 197–206.

**Urbanowicz BR**, **Peña MJ**, **Ratnaparkhe S**, ***et al.* 2012**. 4-O-methylation of glucuronic acid in Arabidopsis glucuronoxylan is catalyzed by a domain of unknown function family 579 protein. *Proceedings of the National Academy of Sciences, USA* **109**: 14253–14258.

**Vain T**, **Crowell EF**, **Timpano H**, ***et al.* 2014**. The cellulase KORRIGAN is part of the cellulose synthase complex. *Plant Physiology* **165**: 1521–1532.

**Vandavasi VG**, **Putnam DK**, **Zhang Q**, ***et al.* 2016**. A structural study of CESA1 catalytic domain of Arabidopsis cellulose synthesis complex: evidence for CESA trimers. *Plant Physiology* **170**: 123–135.

**Vanholme R**, **Demedts B**, **Morreel K**, **Ralph J**, **Boerjan W. 2010**. Lignin biosynthesis and structure. *Plant Physiology* **153**: 895–905.

**Vanholme R**, **Storme V**, **Vanholme B**, ***et al.* 2012**. A systems biology view of responses to lignin biosynthesis perturbations in Arabidopsis. *The Plant Cell* **24**: 3506–3529.

**Vargas L**, **Cesarino I**, **Vanholme R**, ***et al.* 2016**. Improving total saccharification yield of Arabidopsis plants by vessel-specific complementation of caffeoyl shikimate esterase (cse) mutants. *Biotechnology for Biofuels* **9**: 139.

**Viotti C**, **Bubeck J**, **Stierhof Y-D**, ***et al.* 2010**. Endocytic and secretory traffic in Arabidopsis merge in the trans-Golgi network/early endosome, an independent and highly dynamic organelle. *The Plant Cell* **22**: 1344–1357.

**Vukašinović N**, **Oda Y**, **Pejchar P**, ***et al.* 2017**. Microtubule-dependent targeting of the exocyst complex is necessary for xylem development in Arabidopsis. *New Phytologist* **213**: 1052–1067.

**Wang J**, **Howles PA**, **Cork AH**, **Birch RJ**, **Williamson RE. 2006**. Chimeric proteins suggest that the catalytic and/or C-terminal domains give CesA1 and CesA3 access to their specific sites in the cellulose synthase of primary walls. *Plant Physiology* **142**: 685–695.

**Wang P**, **Chen X**, **Goldbeck C**, **Chung E**, **Kang B-H. 2017**. A distinct class of vesicles derived from the *trans*-Golgi mediates secretion of xylogalacturonan in the root border cell. *The Plant Journal* **92**: 596–610.

**Wang Y**, **Bouchabké-Coussa O**, **Le Bris P**, ***et al.* 2015**. LACCASE 5 is required for lignification of the *Brachypodium distachyon* culm. *Plant Physiology* **168**: 192–204.

**Watanabe Y**, **Meents MJ**, **McDonnell LM**, ***et al.* 2015**. Visualization of cellulose synthases in Arabidopsis secondary cell walls. *Science* **350**: 198–203.

**Wightman R**, **Turner SR. 2008**. The roles of the cytoskeleton during cellulose deposition at the secondary cell wall. *The Plant Journal* **54**: 794–805.

**Wightman R**, **Marshall R**, **Turner SR. 2009**. A cellulose synthase-containing compartment moves rapidly beneath sites of secondary wall synthesis. *Plant and Cell Physiology* **50**: 584–594.

**Worden N**, **Park E**, **Drakakaki G. 2012**. Trans-Golgi network – an intersection of trafficking cell wall components. *Journal of Integrative Plant Biology* **54**: 875–886.

**Wu A-M**, **Rihouey C**, **Seveno M**, ***et al.* 2009**. The Arabidopsis IRX10 and IRX10-LIKE glycosyltransferases are critical for glucuronoxylan biosynthesis during secondary cell wall formation. *The Plant Journal* **57**: 718–731.

**Wu A-M**, **Hörnblad E**, **Voxeur A**, ***et al.* 2010**. Analysis of the Arabidopsis IRX9/IRX9-L and IRX14/IRX14-L pairs of glycosyltransferase genes reveals critical contributions to biosynthesis of the hemicellulose glucuronoxylan. *Plant Physiology* **153**: 542–54.

**Xiong G**, **Li R**, **Qian Q**, ***et al.* 2010**. The rice dynamin-related protein DRP2B mediates membrane trafficking, and thereby plays a critical role in secondary cell wall cellulose biosynthesis. *The Plant Journal* **64**: 56–70.

**Yamaguchi M**, **Mitsuda N**, **Ohtani M**, **Ohme-Takagi M**, **Kato K**, **Demura T. 2011**. VASCULAR-RELATED NAC-DOMAIN7 directly regulates the expression of a broad range of genes for xylem vessel formation. *The Plant Journal* **66**: 579–590.

**Yang F**, **Mitra P**, **Zhang L**, ***et al.* 2013**. Engineering secondary cell wall deposition in plants. *Plant Biotechnology Journal* **11**: 325–335.

**Yang J-S**, **Valente C**, **Polishchuk RS**, ***et al.* 2011**. COPI acts in both vesicular and tubular transport. *Nature Cell Biology* **13**: 996–1003.

**York WS**, **O'Neill MA. 2008**. Biochemical control of xylan biosynthesis – which end is up? *Current Opinion in Plant Biology* **11**: 258–265.

**Young RE**, **McFarlane HE**, **Hahn MG**, **Western TL**, **Haughn GW**, **Samuels AL. 2008**. Analysis of the Golgi apparatus in Arabidopsis seed coat cells during polarized secretion of pectin-rich mucilage. *The Plant Cell* **20**: 1623–1638.

**Zeng W**, **Jiang N**, **Nadella R**, **Killen TL**, **Nadella V**, **Faik A. 2010**. A glucurono(arabino)xylan synthase complex from wheat contains members of the GT43, GT47, and GT75 families and functions cooperatively. *Plant Physiology* **154**: 78–97.

**Zeng W**, **Lampugnani ER**, **Picard KL**, ***et al.* 2016**. Asparagus IRX9, IRX10, and IRX14A are components of an active xylan backbone synthase complex that forms in the Golgi apparatus. *Plant Physiology* **171**: 93–109.

**Zhang B**, **Zhang L**, **Feng Li**, ***et al.* 2017**. Control of secondary cell wall patterning involves xylan deacetylation by a GDSL esterase. *Nature Plants* **3**: 17017.

**Zhang D**, **Hrmova M**, **Wan C-H**, ***et al.* 2004**. Members of a new group of chitinase-like genes are expressed preferentially in cotton cells with secondary walls. *Plant Molecular Biology* **54**: 353–372.

**Zhang GF**, **Staehelin LAS. 1992**. Functional compartmentation of the Golgi apparatus of plant cells. *Plant Physiology* **99**: 1070–1083.

**Zhang Y**, **Nikolovski N**, **Sorieul M**, ***et al.* 2016**. Golgi-localized STELLO proteins regulate the assembly and trafficking of cellulose synthase complexes in Arabidopsis. *Nature Communications* **7**: 11656.

**Zhao Q. 2016**. Lignification: flexibility, biosynthesis and regulation. *Trends in Plant Science* **21**: 713–721.

**Zhao Q**, **Nakashima J**, **Chen F**, ***et al.* 2013**. LACCASE is necessary and nonredundant with PEROXIDASE for lignin polymerization during vascular development in Arabidopsis. *The Plant Cell* **25**: 3976–3987.

**Zhong R**, **Morrison WH**, **Freshour GD**, **Hahn MG**, **Ye Z-H. 2003**. Expression of a mutant form of cellulose synthase AtCesA7 causes dominant negative effect on cellulose biosynthesis. *Plant Physiology* **132**: 786–795.

**Zhong R**, **Burk DH**, **Morrison WH**, **Ye Z-H. 2004**. FRAGILE FIBER3, an Arabidopsis gene encoding a type II inositol polyphosphate 5-phosphatase, is required for secondary wall synthesis and actin organization in fiber cells. *The Plant Cell* **16**: 3242–3259.

**Zhong R**, **Peña MJ**, **Zhou G-K**, ***et al.* 2005**. Arabidopsis fragile fiber8, which encodes a putative glucuronyltransferase, is essential for normal secondary wall synthesis. *The Plant Cell* **17**: 3390–3408.

**Zhong R**, **Teng Q**, **Haghighat M**, ***et al.* 2016**. Cytosol-localized UDP-xylose synthases provide the major source of UDP-xylose for the biosynthesis of xylan and xyloglucan. *Plant and Cell Physiology* **58**: 156–174.